EUR 431.e

EUROPEAN ATOMIC ENERGY COMMUNITY - EURATOM

SOLID STATE NEUTRON DETECTOR

by

S. AMELINCKX (C.E.N.), R. DE CONINCK (C.E.N.),
M. DENAYER (C.E.N.), A. GIJS (C.E.N.),
M. HEERSCHAP (EURATOM), P. NAGELS (C.E.N.),
and L. VAN GOOL (C.E.N.)

1964

LEGAL NOTICE

This document was prepared under the sponsorship of the Commission of the European Atomic Energy Community (EURATOM).

Neither the EURATOM Commission, its contractors nor any person acting on their behalf :

1° — Make any warranty or representation, express or implied, with respect to the accuracy, completeness, or usefulness of the information contained in this document, or that the use of any information, apparatus, method, or process disclosed in this document may not infringe privately owned rights; or

2° — Assume any liability with respect to the use of, or for damages resulting from the use of any information, apparatus, method or process disclosed in this document.

EUR 431.e

SOLID STATE NEUTRON DETECTOR by S. AMELINCKX, R. DE CONINCK, M. DENAYER, A. GIJS (C.E.N.), M. HEERSCHAP (EURATOM), P. NAGELS and L. VAN GOOL (C.E.N.).

The object of this research program is to develop a neutron detector for the detection of high neutron fluxes at high temperatures thereby using the SiC diodes.

A number of grown SiC p-i-n junctions, obtained from the Philips Research Laboratories, have been irradiated in the BR1 reactor. The change of their electrical characteristics and of the short-circuit photo-current can be explained by assuming that the intrinsic region, which is slightly p-doped before irradiation becomes slightly n-doped upon prolonged irradiation, hereby reaching a

relatively low limiting value of electron concentration. This would correspond
to a shift of the Fermi-level of the intrinsic region to a position in the lower
part of the upper half of the forbidden energy gap. Not much annealing is found
on measuring the change of the electrical characteristics upon pulse annealing.
Because of the smallness of the width of the space-charge layer (about 1
micron), the grown SiC diodes could not be used as detectors.

In order to obtain a fundamental understanding of the influence of the
defects introduced upon fast neutron irradiation on the electronic behaviour
of SiC, radiation damage studies have also been made on p- and n-type single
crystals of SiC by means of resistivity and Hall effect measurements. Upon
neutron bombardment p-type SiC is converted to n-type material. This indi-
cates that the predominant defect is an effective donor state which is located
at about 0.24 eV below the conduction band. The n-doped material remains of
the same type after various periods of exposure.

The relaxation processes of defects during heat treatment have been exami-
ned by the isochronal pulse annealing technique. No measurable annealing
occurs below 400 ºC. Photospectrometric measurements on the other hand
reveal an annealing process starting at 300 ºC.

EUR 431.e

EUROPEAN ATOMIC ENERGY COMMUNITY - EURATOM

SOLID STATE NEUTRON DETECTOR

by

S. AMELINCKX (C.E.N.), R. DE CONINCK (C.E.N.),
M. DENAYER (C.E.N.), A. GIJS (C.E.N.),
M. HEERSCHAP (EURATOM), P. NAGELS (C.E.N.),
and L. VAN GOOL (C.E.N.)

1964

Supervisor	:	S. Amelinckx (S.C.K.)
Research Associates	:	M. Heerschap (Euratom)
		P. Nagels (S.C.K.)
		R. De Coninck (S.C.K.)
		M. Denayer (S.C.K.)
Technical Assistance	:	A. Gijs (S.C.K.)
		L. Van Gool (S.C.K.)

<p style="text-align:center">*   *   *</p>

TABLE OF CONTENTS

LIST OF FIGURES

*   *   *

SOLID STATE NEUTRON DETECTOR

SUMMARY

        The object of this research program is to develop a neutron detector for the detection of high neutron fluxes at high temperatures thereby using the SiC diodes .

        A number of grown SiC p-i-n junctions, obtained from the Philips Research Laboratories, have been irradiated in the BR1 reactor . The change of their electrical characteristics and of the short-circuit photocurrent can be explained by assuming that the intrinsic region, which is slightly p-doped before irradiation, becomes slightly n-doped upon prolonged irradiation hereby reaching a relatively low limiting value of electron concentration . This would correspond to a shift of the Fermi level of the intrinsic region to a position in the lower part of the upper half of the forbidden energy gap . Not much annealing is found on measuring the change of the electrical characteristics upon pulse annealing . Because of the smallness of the width of the space-charge layer (about 1 micron) the grown SiC diodes could not be used as detectors .

        In order to obtain a fundamental understanding of the influence of the defects introduced upon fast neutron irradiation on the electronic behaviour of SiC, radiation damage studies have also been made on p- and n-type single crystals of SiC by means of resistivity and Hall effect measurements . Upon neutron bombardment p-type SiC is converted into n-type material . This indicates that the predominant defect is an effective donor state which is located at about 0.24 eV below the conduction band . The n-doped material remains of the same type after various periods of exposure .

        The relaxation processes of defects during heat treatment have been examined by the isochronal pulse annealing technique . No measurable annealing occurs below $400°C$. Photospectrometric measurements on the other hand reveal an annealing process starting at $300°C$.

1. INTRODUCTION

        The object of this research program is to develop a neutron detector for the detection of high neutron fluxes at high temperatures thereby using SiC as a base material . From the fact that SiC p-n junctions still maintain their rectifying properties at 500°C and that a rather high photovoltage develops upon gamma irradiation we concluded that it might be possible to develop a SiC neutron detector meeting the above requirements .

The range of α-particles in SiC is of the order of some tens of microns . With respect to the signal-noise ratio especially at 500°C the depth of the p-n irradiation chamber has to be of the same order of magnitude thereby aiming at a high efficiency of charge collection ; this efficiency depends on the reverse voltage, the mobility and the lifetime of the charge carriers .

Large single crystals of SiC are grown in a Lely furnace from technical grade SiC . The impurity content, mainly consisting of Al, which is acting as an acceptor, is of the order of $10^{18}/cm^3$. The acceptors are partly compensated by N_2, which is acting as a donor . By overcompensating the Al impurities by N_2 during the process of growth of the crystals a p-n ionization chamber is formed of which the impurity content of the n-conduction part is of the order of $10^{19}/cm^3$. On basis of the behaviour of the electrical characteristics it is supposed that the p-n junction has a p-i-n structure . From the magnitude of the extrapolated saturation current, we concluded that the width of the ionization chamber is of the order of the diffusion length i.e. about 1 micron thereby taking a mobility of 100 $cm^2/V.s$ and a lifetime of 10^{-8} s .

The depth of these grown p-n junctions, which are deep-lying, is too small to be of practical importance .
The width of the space-charge layer can be extended by diminishing the impurity content by several orders of magnitude and/or by applying the ion-drift techniques of PELL [1]. The last possibility has not been examined so far by the Philips Research Laboratories whereas the best single crystals of sufficient size have still an impurity concentration of about $10^{17}/cm^3$.

The alternative is to make p-n ionization chambers at the surface of the crystals, for instance by diffusion of acceptor impurities in n-conductive crystals. The width of the space-charge layer can be made of sufficient magnitude by using crystals of high purity and/or applying the PELL mechanism thereby running into the same difficulties as mentioned for grown p-n junctions .

However, the junction can be of the order of some tens of microns in creating a graded junction by suitable diffusion techniques as can be demonstrated by etching techniques .

The Philips Research Laboratories obtained in the mean time a substantial amount of knowledge about the diffusion technique . The production of p-n barriers of sufficient quality, however, is still under examination . A change of the research program slowed down the progress so considerably that we decided not to prolong the contract . The electronics for the detection of particles as well as related apparatus as for the measurements of the capacity and the lifetime will not be reviewed here . Quite an effort is made to study the radiation damage and annealing process by measuring the change of the electrical characteristics of grown p-n junctions and by Hall, resistivity and photospectrometric measurements of homogeneous material . These measurements and their theoretical explanations are all reviewed in the next paragraph along with the apparatus for irradiation of crystals, the automatic recording of the electrical characteristics and the Hall and resistivity apparatus . They are now used for other purposes as well . Part of these measurements, especially the Hall, resistivity and photospectrometric measurements, will be continued after the end of the contract .

The aim of the resistivity and Hall effect measurements was to obtain a fundamental understanding of the influence of the defects introduced upon fast neutron irradiation on the electronic behaviour and to establish the reasons for the deterioration of the semiconductor devises . Radiation damage studies on homogeneous material of SiC were started on n- and p-type material . What is described here is a report on an investigation still going on, so that no complete picture of the various problems can be given . The first results indicated that p-type SiC is converted into n-type upon neutron irradiation . So, it can be concluded that the predominant defect produced by this bombardment is an effective donor state which is located at about 0.24 eV below the conduction band . The n-type material remained of the same type after various periods of exposure .

An exact value for the number of defects produced for a given bombardment cannot be given . However, from the measurements the conclusion can be drawn that

the ability of SiC to withstand radiation damage is not better than for germanium
or silicon.

The relaxation processes of defects during heat treatment have been exa-
mined by an isochronal pulse annealing technique. It has been found that no mea-
surable annealing of the neutron bombarded material occurs below 400°C. From the
Hall and resistivity measurements it follows as well that upon irradiation with a
flux of less than 10^{15} nvt_f the n- and p-conductive parts of the p-n junctions will
not be affected by fast neutron irradiation so that the change of the electrical
characteristics is governed only by a shift of the Fermi level of the intrinsic or
nearly intrinsic region. From the change of the characteristics we concluded that
the electron concentration is approaching a relatively low limiting value upon pro-
longed irradiation so that the Fermi level is approaching a position in the lower
part of the upper half of the forbidden energy gap.

Not much annealing is found on measuring the change of the electrical cha-
racteristics upon pulse annealing. Above 800°C one has to be careful in drawing
conclusions as is demonstrated by a change of the electrical characteristics.
The photospectrometric measurements on the other hand reveal an annealing process
starting at 300°C as far as the short wave-length of the spectrum is concerned.
At 900°C a residue is still left.

2. RADIATION DAMAGE AND ANNEALING STUDIES OF GROWN SiC p-n JUNCTIONS

2.1. Irradiation facility

An oven allowing to reach temperatures up to 500°C and to be inserted
into a vertical channel of reactor BR1 was constructed.

The aims of the oven are :

1) to create the possibility of measuring radiation damage at constant tempera-
   tures so that semiconductor temperature effects are eliminated ;

2) to examine at which temperature the radiation damage rate may eventually be
   balanced by the annealing rate.

The oven (Fig. 1) is composed of three parts : the reactor plug filled
with lead, boron and paraffin, the guide tube and the oven itself whose parts can
easily be separated. The whole construction is of pure aluminium (99.99 %).
The temperature is measured inwards and outwards with iron-constantan thermocouples.
The heater (80 % Ni and 20 % Cr) which is wound on a pyrofilite core is about 300
ohms. The sample with its two measuring wires can be inserted or withdrawn during
the working period of the reactor by sliding it through a helically wound aluminium
inner tube. The construction of the lower part of the guide tube is such that all
oven wires can easily be connected or disconnected.

The electronic apparatus consists of the oven regulation and control sup-
ply with the temperature measuring set.

2.2. Voltage-current characteristics measuring circuit

A circuit (Fig. 2) is constructed whereby the voltage-current characteristics of p-n junctions are drawn automatically by an X-Y recorder.

The voltage across R_s is proportional to the current through the diode, while over the resistor R_2 part of the voltage over the junction plus the voltage over R_s is measured. For a total voltage of 100 V across the diode, the error in voltage measurement due to additional voltage over R_s is only 5 mV upon 100 V (5 mV is the F.S.D. of the recorder) i.e. an error of 5×10^{-5}. For a voltage of 1 V the error is still only 0.5 %. For voltages of 1 V or less the full scale deflection is not always reached so that the total error can always be kept below 0.5 to 1 %.

The greatest advantage of this system lies in the fact that, as well as the power supply, the two inputs X and Y can be grounded. Thereby, the bleeder $R_{p1} - R_{p2}$ should not be made of very high resistors because it does not affect the current or voltage through the diode. Several curves can be drawn on the same paper so that changes can easily be followed.

2.3. The change of the electrical characteristics and of the photocurrent of grown SiC p-n junctions upon reactor irradiation at 80°C

Several SiC p-n junctions which are grown in a Lely furnace and whose properties are described by GREEBE and KNIPPENBERG [2] [3] have been irradiated in the BR1 reactor. The change of the characteristics and the short-circuit photocurrent upon reactor irradiation have been measured. The concentration of the acceptors in these crystals is about $10^{18}/cm^3$; their ionization energy is about 0.3 eV. The n-conductive part of the junction is formed by overcompensating the acceptors by nitrogen donor impurities of which the concentration is about $10^{19}/cm^3$ and the ionization energy 0.08 eV. GREEBE and KNIPPENBERG suppose that these junctions have a p-i-n structure, the width of the junction being about equivalent to the diffusion length. Within the range of our irradiation ($< 10^{15}$ nvt$_f$) the amount of irradiation produced defects may be expected to be small compared to the high concentration of chemical impurities already present before irradiation, so that the n- and p-conductive parts of the junction will not be affected by irradiation.

The change of structure of the junction will be governed only by a shift of the Fermi level of the "intrinsic" region and an eventual change of the ratio d/L, where d is the width of the intrinsic region and L is the diffusion length in this region, according to the calculations of HERLET and SPENKE [4].

It has been found so far that p-type SiC single crystals convert into n-type upon reactor irradiation so that the predominant radiation produced defect gives a donor state. The change of the leakage current across the junction upon reactor irradiation (Fig. 4) may be interpreted, however, as a decrease of leakage current across n-type material by assuming that less effective acceptor states are

formed along with the donor states, the electron concentration approaching a relatively low limiting value upon prolonged irradiation.

The gross features of the change of the characteristics which all junctions exhibit upon reactor irradiation, are shown schematically in Fig. 3. The forward characteristic becomes steeper, reaching its steepest position at a dose of about 10^{15} nvt$_f$. The forward current decreases again upon further exposure, rapidly becoming bad at doses of more than 5×10^{15} nvt$_f$. The reverse current and the "foot" [3] on the other hand decrease upon reactor irradiation as is shown in more detail in Fig. 4. Both are partly ascribed to leakage currents across n-type material as already mentioned.

In Fig. 5 is represented the change of the forward current at a constant bias voltage of 2 volts of one on the samples during irradiation in the reactor and of junction Ph − h, the values of which have been borrowed from Fig. 7. In both cases the shape depends on the voltage.
The change of the short-circuit photocurrent upon irradiation with ultraviolet light and brought about by reactor irradiation of a sample junction of series H-75 and of P-15 is shown in Fig. 6.

The change of the photocurrent of the junction of series H-75 may be explained by assuming that it is due to a change of the diffusion length in the "intrinsic" region by a shift of the Fermi level and that the "intrinsic" region is slightly p-doped before irradiation, becoming intrinsic or nearly intrinsic at the maximum photocurrent. The intrinsic region becomes slightly n-doped upon further exposure, the electron concentration approaching a relatively low limiting value. The transition layer of the junction of series P-15, exhibiting no maximum in the photocurrent, may be considered to be intrinsic or nearly intrinsic before irradiation within the range of our irradiations ($< 10^{13}$ nvt$_f$), becoming slightly n-doped upon irradiation.

The forward characteristic is hidden in the low current range by the high leakage current so that the measurements are significant only in an intermediate current range, which is rather narrow. In Fig. 7 is represented the change of the $\ln I$ versus voltage curve of the forward characteristic, after having subtracted the leakage current, of junction Ph-h which is displaying a maximum in the photocurrent curve. The slope of the semi-log plot is $q/1.68$ kT before irradiation, which is that of the transition region between regions with the slopes $q/2kT$ and q/kT. This indicates that the intrinsic region is slightly p-doped, the concentration of the holes being about $10^{12}/cm^3$ as may be estimated from the condition that the current at the transition region of the characteristic is about equivalent to the saturation current of the p^*-p barrier. The slope becomes suddenly q/kT at a dose of 10^{14} nvt$_f$ where the photocurrent reaches its maximum value, which has been considered to occur when the transition layer of the junction becomes intrinsic or nearly intrinsic. The increase of the slope may be explained by assuming that the diffusion length in the intrinsic region has become much larger than the width of this region. Upon further exposure the slope decreases again approaching a limiting value of $q/1.66$ kT.

which is that of a transition region of the forward characteristic, indicating that the "intrinsic" region is slightly n-doped, the concentration of the electrons being about $10^{12}/cm^3$. The decrease of the slope may be due to a decrease of the diffusion length compared to the width of the intrinsic region.

The slope of the semi-log plot of the forward characteristic of junction Ph-i, which displays a photocurrent curve without a maximum, is $q/2.32$ kT before irradiation approaching $q/2$ kT upon prolonged irradiation. The saturation current (intercept with the current axis) increases slowly upon irradiation, approaching a limiting value of 6×10^{-19} A/cm^2 at a dose of 10^{15} nvt_f, which has been found to occur with all junctions. The increase of the saturation current may be due to an increase of d/L, causing an increase of the forward current at a constant bias voltage as is shown in Fig. 5. Upon still further exposure the forward characteristic rapidly becomes bad, which may be due to a further decrease of the diffusion length, so that the voltage drop across the intrinsic region is not negligible anymore.

2.4. Annealing of irradiated SiC p-n junctions

In Fig. 8 and 9 is presented the change of the forward and the reverse characteristic upon pulse annealing. The diode has been irradiated with a dose of 10^{15} nvt_f at 80°C. The pulses are of 30 minutes duration. The reference temperature is 0°C, whereas the diodes are heated under an inert atmosphere.

2.5. Reactor irradiation of grown SiC diodes at a temperature of 500 C

The change of the characteristics is measured during irradiation in the BRI reactor at a temperature of 500°C. A difficulty encountered with this type of measurements is the period of ten to twenty minutes before the temperature of the crystal is stabilized at a temperature of 500°C ; this time is lost for the recording of the characteristics.

The results are represented in Fig. 10 and are expressed as the change in current in the forward direction at a constant voltage of 1.6 volt and the change in reverse current at a bias voltage of 0.9 volt.

No increase in the forward current is observed in contrast to the results at 80°C.

The reverse current remains practically constant from 8×10^{14} to 5×10^{15} nvt_f

Annealing of any importance has not been observed.

A diode which has been subjected to a flux of about 10^{16} nvt_f is heated during 15 minutes at a temperature of 1000°C in its original quartz container and slowly cooled down.

The characteristics were measured, although the time during which the crystal was held at 1000°C was very short. They are represented in Fig. 11 to demonstrate how careful one has to be in drawing conclusions from annealing studies at temperatures above 700 – 800°C.

The decrease in resistance of the diodes is due to surface conduction, which might have been brought about either by deposition of Si, which has been evaporated from the quartz container, or by selective evaporation of Si or C from the SiC surface.

After the diode has been sand-blasted no sign of annealing was observed. The brown coloration has disappeared however.

The change of the photocurrent is measured at a temperature of 500°C during irradiation in the BRI reactor. The result is represented in Fig. 12.

2.6. Photospectrometric measurements

The results of the photospectrometric measurements, which have been obtained so far with the aid of a Beckmann photospectrometer type DK-I, are represented in Fig. 13. The curves are normalized at a wave-length of 2500 mμ. It follows from this figure that between 400 and 800 mμ (width energy gap 400 mμ) colour centres are introduced upon reactor irradiation. They partly anneal out whereas at a temperature of 900°C a residue is still left.
Continuation of these measurements may in correlation with Hall and resistivity measurements give important results concerning the defects introduced upon reactor irradiation and their annealing behaviour.

3. RADIATION DAMAGE IN SINGLE CRYSTALS OF SILICON CARBIDE

3.1. Introduction

In this report a short review will be given of the effects of fast neutrons on the electrical properties of silicon carbide. The crystals used for these experiments were irradiated in the S-92 facility of the BRI research reactor.
The research in this field is still going on, so that no complete picture of the various problems can be given.
An investigation on radiation damage in silicon carbide by fast neutrons has been made by AUKERMAN et al. [5]. They studied the behaviour of SiC diodes upon neutron irradiation and found SiC to be a promising material for device applications in radiation fields.
They observed however, only a slight annealing of the damage after one hour at 320°C.
In view of the annealing behaviour of the change of length of SiC specimens reported by PRIMAK et al. [6] it was expected to have a more rapid recovery at 500°C. The results of this research program are summarized in the following four chapters.
In the first section, a short description of the method and the apparatus used for the measurements will be given. In the second and third part a summary is given of the conductivity and Hall effect measurements carried out on p- and n-type hexagonal silicon carbide before and after irradiation.
Isochronal pulse annealing experiments on irradiated crystals are reported in the last chapter.

3.2. VAN DER PAUW's method

We decided to use VAN DER PAUW's method [7] for measuring the resistivity
and the Hall constant . This method is based upon a theorem which holds for a plane-
parallel sample of arbitrary shape with four small contacts at its circumference
(see Fig. 14) . The specific resistivity can be derived from the measurement of two
pseudo-resistances :

$$R_I = \frac{V_{34}}{I_{12}} \quad \text{and} \quad R_{II} = \frac{V_{13}}{I_{24}}$$

where V_{34} and V_{12} are the potential differences between the contacts 3-4 and 1-3,
and I_{12} resp. I_{24} the current through the contacts 1-2 and 2-4 . It has been shown
by VAN DER PAUW that the specific resistivity is a function only of the two resis-
tances R_I and R_{II} and of the thickness of the platelet d :

$$\rho = \frac{\pi\, d}{\ln 2} \frac{R_I + R_{II}}{2} f \left[\frac{R_I}{R_{II}}\right]$$

The function $f\left[\frac{R_I}{R_{II}}\right]$ is given by VAN DER PAUW in graphical form (Fig. 15) .
Because R_I and R_{II} are measured in different parts of the sample, a change of $\frac{R_I}{R_{II}}$
with temperature indicates that the specimen is not homogeneous .
To reduce the influence of contacts of finite size, and to limit the chance of
meeting inhomogeneities, VAN DER PAUW suggested to use a four leaf clover shaped
sample .
The Hall coefficient can be determined on the sample by measuring the change of the
resistance $R_{III} = \frac{V_{14}}{I_{23}}$ when a magnetic field is applied perpendicularly to the
sample $R_H = 10^8 \times d \times \frac{\Delta R_{III}}{H}$ where H is the magnetic field strength .

3.3. Experimental

The SiC single crystals, of hexagonal structure, were obtained from the
Philips Research Laboratories . They are grown in the Lely furnace using technical
grade silicon carbide as starting material . The p-type conductivity is mainly due
to the presence of aluminium which acts as an acceptor centre . These acceptor le-
vels are partly compensated with nitrogen acting as a donor impurity .
It was found by the Philips Research Laboratories that a Ni-Mo alloy was a good con-
tacting material, showing an ohmic behaviour on n-type material and on p-type mate-
rial after the addition of small amounts of aluminium .
Molybdenum strips spot welded to platinum strips are alloyed in a high-frequency
furnace on four diagonal points of the platelet using the nickel alloy . After this
treatment, the crystals are sand-blasted to clean the surface .

Apparatus

MEASURING CIRCUIT (Fig. 16)

The specific resistivity and Hall constant are determined by means of a
direct-current method and constant magnetic field . The potential differences between

the contacts, to be known according to VAN DER PAUW's method are measured with the aid of a Dieselhorst potentiometer using a galvanometer as zero-detector. An error may be introduced by thermoelectric effect if the temperature of the specimens is not uniform. This error can be eliminated by reversing the current and averaging the two readings. The current, measured with a Microva multirange galvanometer, is delivered by a number of lead accumulators which are placed in a thermostat, in order to eliminate voltage fluctuations. A switching system enables to choose one pair of contacts for the current flow, to reverse the current and to transfer the probe voltage to the measuring circuit.

The Hall effect measurements were performed in a field strength of 5400 gauss.

SPECIMEN HOLDER (Fig. 17).

The specimen holder designed for high temperature measurements consists of an alumina rod with 6 holes which contain four platinum contact wires and a platinum-platinum/rhodium thermocouple. The rod is mounted in a metal head which contains 6 vacuum sealed through-leads and a connection for a high vacuum system. The sample holder is surrounded by an alumina tube which can be evacuated to about 10^{-5} mm Hg.

OVEN AND OVEN REGULATOR (Fig. 18)

The oven consists of a pyrofilite tube which carries a non-inductive winding of platinum wire. The thermal insulation is small so that the oven reaches its equilibrium state in a short time. The temperature has to be kept constant within narrow limits, especially for Hall effect measurements. The oven temperature stabilizer, which has been built, is based on a bridge system in which the oven resistance forms one arm of the bridge.

CRYOSTAT (Fig. 19)

For measurements at low temperatures a metal cryostat has been constructed. This cryostat consists of a central copper tube which carries a heater of constantan wire. The copper tube is in thermal contact via a thin copper sheet with the can that contains the liquid nitrogen. The central tube and the can containing the refrigerant are surrounded by a vacuum jacket. By adjusting the current through the heater, the temperature can be varied continuously between liquid nitrogen and room temperature.

3.4. Resistivity and Hall constant measurements of SiC single crystals

Extensive studies on the electrical properties of SiC single crystals were made by BUSCH [8], BUSCH and LABHART [9], LELY and KRÖGER [10] and by VAN DAAL, KNIPPENBERG and WASSCHER [11] [12] [13] of the Philips Research Laboratories. BUSCH and LABHART determined the temperature dependence of the resistivity and Hall constant in a temperature range from 100° to 1100°K for n-type (green) and p-type (black) silicon carbide found among the commercial crystals. They noticed a maximum

in the Hall mobility for both type of crystals, at about 300°K. The decrease in mobility towards lower temperatures was attributed to a transition to impurity band conduction.

The electrical behaviour of pure n- and p-type single crystals of SiC doped with nitrogen and aluminium during growth in the Lely furnace was investigated by LELY and KRÖGER. They determined the energy levels of the impurities added to the crystals :

- the depth of the N donor level lies in between 0.06 and 0.085 eV below the conduction band ;

- the ionization energy for the Al impurity is about 0.27 eV.

Continuing the work of LELY and KRÖGER, VAN DAAL and co-workers made an extensive study of the electronic conduction in p-type SiC between 300° and 1500°K. They explained the temperature dependence of the Hall mobility as a consequence of different scattering mechanisms, e.g. optical, acoustical, piezoelectric and impurity scattering.

A first aim of our Hall effect and resistivity measurements was to compare our results with those obtained by H.J. VAN DAAL on specimens of the same growth.

The agreement was very good.

p-TYPE SILICON CARBIDE

The specific resistivity and Hall coefficient of a number of p-type single crystals of SiC were determined in a temperature range from 300°K to 1300°K. Fig. 20 shows the logarithm of the conductivity of three of these crystals as a function of the inverse temperature.

In Fig. 21 the number of free holes is plotted versus the inverse temperature. The concentration of the free holes has been calculated from the Hall coefficient R using the classical formula $p = \frac{3}{8} \frac{\pi}{Re} \frac{1}{}$. The curves of log p vs. $\frac{1}{T}$ can be interpreted as follows : the straight part at intermediate temperatures is connected with the liberation of charge carriers from impurity centres, which causes the exponential change of the free hole concentration with $\frac{1}{T}$.

At high temperatures p tends to a constant value $N_A - N_D$, due to the exhaustion of the acceptors. The bending of the conductivity curves at high temperatures is then also explained in the same way : constant number of charge carriers and reduction of the mobility with increasing temperature.

In Fig. 22 we have plotted log $\left[\frac{10^3}{T}\right]^{3/2}$ p as a function of the inverse temperature. From the slope of the straight parts of these curves the activation energy of the impurity centres has been deduced. Furthermore, a graphical analysis of these curves developed by VAN DAAL et al. enables us to evaluate the number of acceptors N_A and donors N_D. This method is based on the formula for partly compensated acceptor levels :

$$\frac{p (p + N_D)}{N_A - N_D - p} = N_V g^{-1} e^{-\frac{\varepsilon}{kT}}$$

where   p = number of free holes

N_A = number of acceptors

N_D = number of donors

N_v = density of states

g = multiplicity ratio between valence band and acceptor level.

In Fig. 23 the Hall mobility is given as a function of the absolute temperature. At 300°K μ lies between 28 and 42 cm^2 V^{-1} s^{-1} for the different crystals. The mobility decreases with increasing temperature and becomes about 2.7 cm^2 V^{-1} s^{-1} at 1000°K.

The most important data which can be deduced from the curves are collected in Table I.

TABLE I

	Activation energy eV	Mobility cm^2 V^{-1} s^{-1} at 300°K	Mobility cm^2 V^{-1} s^{-1} at 1000°K	N_A 10^{18} cm^{-3}	N_D 10^{18} cm^{-3}	N_D/N_A
1	0.31	42	2.8	10	2	0.2
2	0.32	28	2.6	4.2	0.7	0.17
3	0.31	34	-	-	-	-
4	0.20	37	2.8	16	2.8	0.16
5	0.26	28	3.0	11	5.7	0.50

VAN DAAL has made a complete analysis of the Hall mobility curves in p-type crystals. The temperature dependence of the Hall mobility can be explained by assuming the presence of different scattering mechanisms scattering by optical phonons, acoustical mode, piezoelectrical, and impurity scattering.

In Fig. 24 we have plotted reciprocal Hall mobility for the three crystals as a function of the inverse temperature. The full lines represent the experimentally found values. The broken lines represent the theoretical curves for scattering by optical phonons (e$^{\frac{\theta}{T}}$ – 1). In the temperature range between 300°K and 450 K the experimentally found Hall mobility curve coincides well with the theoretical curve for scattering of holes by optical phonons.

n-TYPE SILICON CARBIDE

The conductivity and electron concentration curves (Fig. 25) of the n-type single crystals have the same shape as the p-type specimens. As a consequence however, of the lower activation energy of the donor impurities (about 0.08 eV) the maximum in the conductivity is reached at a lower temperature.

The Hall mobility of the electrons (Fig. 26) goes over a maximum at 250°K. For lower temperatures there is a very steep drop, which has been interpreted by BUSCH and LABHART as a transition to impurity band conduction. At room temperature μ is of the order of 200 cm^2 V^{-1} s^{-1}, which is about a factor of five higher than for the p type crystals.

3.5. Neutron irradiation of SiC single crystals

Resistivity and Hall coefficient measurements as a function of tempera-
ture have been performed on one n-type and three p-type single crystals of SiC af-
ter irradiation in the BRI reactor .

n-TYPE SILICON CARBIDE

The n-type single crystal, used for the exposure, had a donor concentra-
tion of about 3×10^{17} atoms cm^{-3}, a mobility of 183 cm^2 V^{-1} s^{-1} at room temperature
and an activation energy of 0.065 eV for the donor impurities (calculated from the
slope of the log n vs. $\frac{1}{T}$ curve) . It was irradiated in the BRI reactor at reactor
temperature (80'C) with an integrated fast neutron flux nvt$_f$ = 3.8×10^{16} cm^{-2} .
After exposure the resistivity was measured as a function of temperature in the
range from 300 to 700"K . A semi-log plot of the specific conductivity vs. recipro-
cal temperature before and after irradiation is shown in Fig. 27 . It was found
that the resistivity was markedly increased upon irradiation . The slope of the
log σ vs. $\frac{1}{T}$ curve corresponds to an energy of about 0.47 eV (calculated using the
formula $e^{-\frac{\Delta E}{kT}}$) . This value, or twice this value, represents the depth of the
electron traps introduced in n-type SiC upon fast neutron irradiation . The Hall
coefficient was determined at only one temperature, 550"K . This measurement indi-
cates that the specimen remained n-type material after the exposure nvt$_f$ = $3.8 \times$
10^{16} cm^{-2} . The Hall mobility in the n-type single crystal is decreased by a factor
of two upon irradiation .
Before exposure the mobility at 550°K is 70 cm^2 V^{-1} s^{-1} . It is decreased to 33 cm^2
V^{-1} s^{-1} after irradiation, resulting from additional scattering by the newly intro-
duced lattice defects .

p-TYPE SILICON CARBIDE

Three p-type single crystals were given an exposure of nvt$_f$ = 2.2×10^{17} cm^{-2}
at reactor temperature . The electrical properties of these crystals before neutron
bombardment are summarized in Table 2 .

TABLE 2

Specimen	N_A $\times 10^{-18}$cm^{-3}	N_D $\times 10^{-18}$cm^{-3}	σ Ω^{-1} cm^{-1} at 300°K$\times 10^2$	Hole conc. at 300"K $\times 10^{-15}$cm^{-3}	Mobility cm^2 V^{-1}s^{-1} at 300"K	ΔE eV
1	10	2	0.94	1.7	42	0.3
2	11	5.7	1.6	3.6	28	0.26
3	16	2.8	30	57	37	0.20

The activation energy for the acceptor centres is calculated from the slope of the
log p $\left[\frac{10^3}{T}\right]^{3/2}$ vs. $\frac{1}{T}$ curve .

Fig. 28 and 29 show the temperature dependence of the specific conductivity of spe-
cimens 1 and 2 after reactor irradiation in the temperature range from 300° to 700°K.
As in the case of n-type SiC the resistivity was markedly increased after irradiation.
For specimen 1 the slope of the log σ vs. $\frac{1}{T}$ curve is nearly linear over the whole
temperature range, indicating one group of defects. This slope corresponds to an
ionization energy of about 0.24 eV. However, the bending of the conductivity curve
of specimen 2 suggests that more levels could be present.
The Hall coefficient as a function of temperature was determined on one p-type
single crystal (specimen 1).
In Fig. 28 the free carrier concentration is plotted against the inverse temperature.

The measurement indicates that p-type SiC is converted to n-type SiC by
the action of the defects introduced by fast neutron irradiation. Here a difficulty
arises since the contacts on the irradiated specimen were these that are ohmic, on
p-type material. Non-ohmic behaviour generally results in rectifying properties of
the contacts. The influence of the contacts on the irradiated p-type material has
to be further investigated.

The log n vs. $\frac{1}{T}$ curve has a linear slope which corresponds to an activa-
tion energy of 0.20 eV or twice this value. At 380°K the p-type sample had a hole
concentration of 3×10^{16} cm^{-3}. As a result of the neutron bombardment an n-type
sample with an electron concentration of 4×10^{12} cm^{-3} at the same temperature is
obtained. The mobility of the irradiated p-type material has a rather unusual be-
haviour. The mobility was slightly greater after exposure : before irradiation
$\mu = 26$ cm^2 V^{-1} s^{-1} at 380°K, after irradiation $\mu = 32$ cm^2 V^{-1} s^{-1} at 380°K.
Increase in temperature from 380°K to 700°K (Fig. 30) results in a further increase
in mobility. An explanation of this behaviour cannot yet be given. After the first
temperature cycle to 700°K the resistivity of the irradiated specimens seemed to in-
crease. This effect was found in the case of other semiconductors as e.g. germanium
after neutron irradiation and was explained as a results of clustering of defects.
Four new contacts were alloyed on samples 2 and 3 in the high-frequency furnace.
After this thermal treatment (2 min at 1500°C) the specimens were again p-type and
the original conductivity and hole concentration were nearly restored (Fig. 29).

3.6. Pulse annealing in p- and n-type SiC after neutron exposure

In order to investigate the relaxation processes of defects during heat
treatment, pulse annealing experiments were performed on the irradiated specimens
on which Hall- and resistivity measurements were carried out as a function of tem-
perature.
Extensive studies of annealing of radiation damage, performed on a number of semi-
conductors, have shown that several complex relaxation processes can occur ; in many
cases interpretation is very difficult. However, these annealing experiments have
yielded information about the nature of defects produced by irradiation and on the
mechanism of their removal.

The pulse annealing experiments were carried out on the n-type single crystal, which has received a fast neutron dose $nvt_f = 3.8 \times 10^{16}$ cm^{-2}, and on one p-type crystal (specimen 1) to which an exposure of $nvt_f = 2.2 \times 10^{17}$ cm^{-2} was given. Isochronal temperature pulses of about 30 minutes were given in the temperature range between 100 and 900°C, the conductivity and Hall coefficient were then measured at a reference temperature.

p-TYPE SILICON CARBIDE

The results of the pulse annealing experiment are shown in Fig. 31 ; the conductivity of the specimen was determined at the pulse temperature and at a reference temperature of 18.5°C. This curve reveals that no recovery in conductivity is observed below 400°C.

The recovery of the conductivity as a function of the annealing temperature is shown in Fig. 32. It can be seen that measurable annealing occurs above 400°C. After this thermal cycle the conductivity is increased by about two orders of magnitude but the original conductivity of the specimen, before irradiation $\sigma = 9.4 \times 10^{-3}$ ohm^{-1} cm^{-1} at room temperature, is far from being restored.

The Hall coefficient of the converted p-type sample was determined only at the pulse temperature. The free carrier concentration as a function of the inverse value of the annealing temperature is shown in Fig. 33. Here again a marked increase in the free carrier concentration, associated with the removal of defects is found above 400°C. The original p-type material, converted into n-type by irradiation, remained n-conductive during the whole heat treatment.

n-TYPE SILICON CARBIDE

The results of pulse annealing for the n-type specimens are shown in Fig. 34 and 35. Here a reference temperature of 290°C has been chosen for the measurements of the conductivity and the Hall coefficient. The recovery of conductivity and electron concentration as a function of the pulse temperature is shown in Fig. 36. The annealing behaviour of the n-type specimen seems to be essentially the same as that of the converted p-type sample. It can be concluded that only above 400°C a release of trapped electrons occurs, followed by disappearance of the electron traps.

Further investigations about the isothermal annealing of irradiated silicon carbide, in order to study the activation energy for motion of the mobile defects and the nature of defects, will be performed.

REFERENCES

[1] E.M. PELL :
   J. Appl. Phys. 31, 291 (1960)

[2] C.A.A.J. GREEBE and W.F. KNIPPENBERG :
   Philips Res. Repts. 15, 120 (1960)

[3] C.A.A.J. GREEBE and W.F. KNIPPENBERG :
   Philips Res. Repts. 16, 389 (1961)

[4] A. HERLET and E. SPENKE :
   Z. Ang. Phys. 7, 9, 149, 195 (1955)

[5] L.W. AUKERMAN, A.C. GORTON, R.K. WILLARDSON and V.E. BRYSON :
   Silicon Carbide, Pergamon Press p. 388

[6] W. PRIMAK, L.A. FUCKS and P.P. DAY :
   Phys. Rev. 103, 1184 (1956)

[7] L. VAN DER PAUW :
   Philips Res. Repts. 13, 1 (1958)

[8] G. BUSCH :
   Helv. Phys. Acta 79, 463 (1946)

[9] G. BUSCH and H. LABHART :
   Helv. Phys. Acta 19, 463 (1946)

[10] J.A. LELY and F.A. KRÖGER :
   Halbleiter und Phosphore,
   Verträge des internationalen Kolloquium 1956 Garmisch-Partenkirschen (1958)

[11] H.J. VAN DAAL, J.D. WASSCHER and W.F. KNIPPENBERG :
   Conference on Diamond Physics, Reading (1960)

[12] H.J. VAN DAAL, C.A. GREEBE, W.F. KNIPPENBERG and H.J. VINK :
   J. Appl. Phys. 32, 2225 (1961)

[13] H.J. VAN DAAL, W.F. KNIPPENBERG and J.D. WASSCHER :
   On the Electronic Conduction of SiC Crystals between 300 and 1500° K
   In the press

*   *   *

OVEN

2901

192

197

0 1 2 cm

REACTOR PLUG

Sample Inlet

2110

Lead
+Paraffin
+Boron

Fig. 1
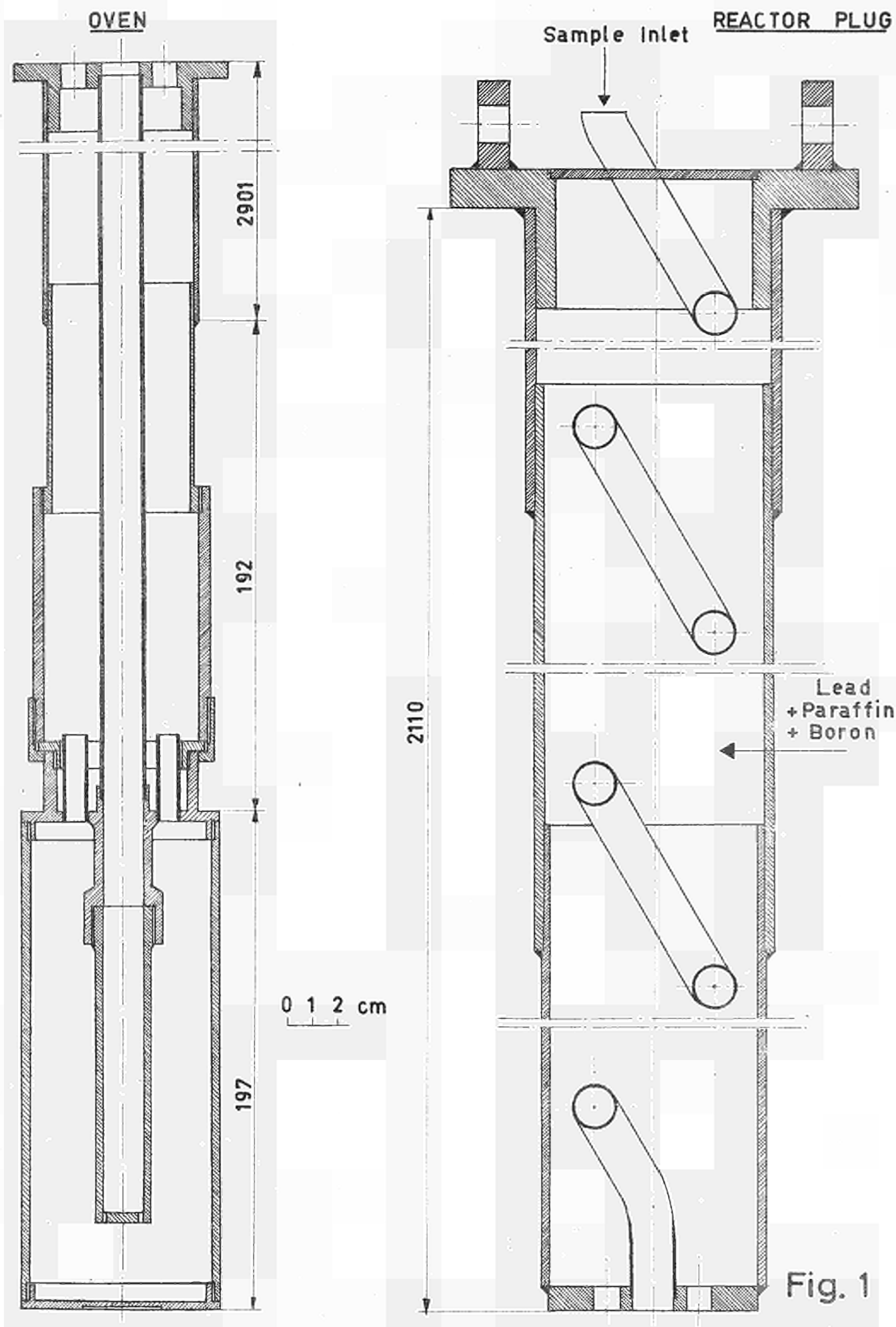
Schematic view of the oven in the BR1 reactor.

C/349/63

Voltage-current characteristics measuring-circuit.

Fig. 2

Fig. 3
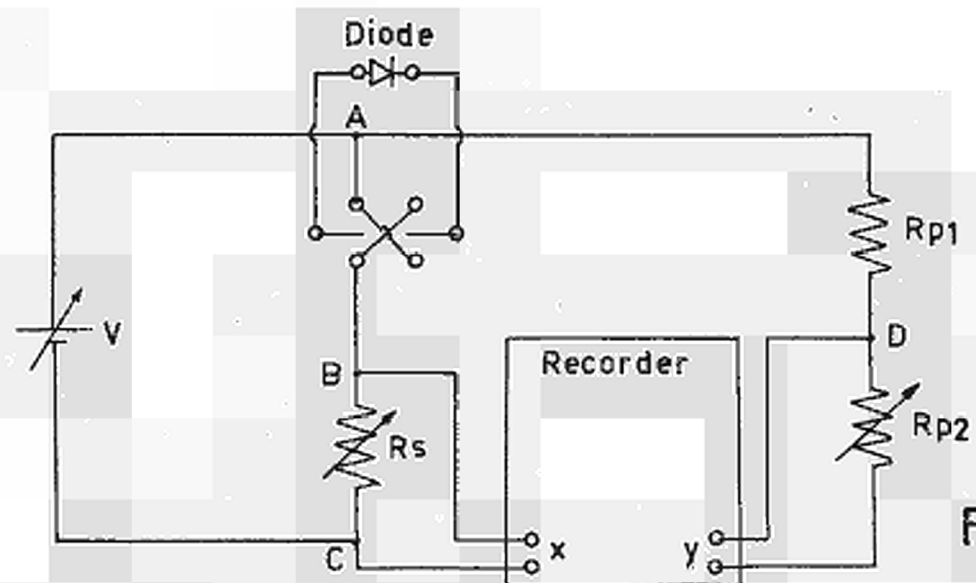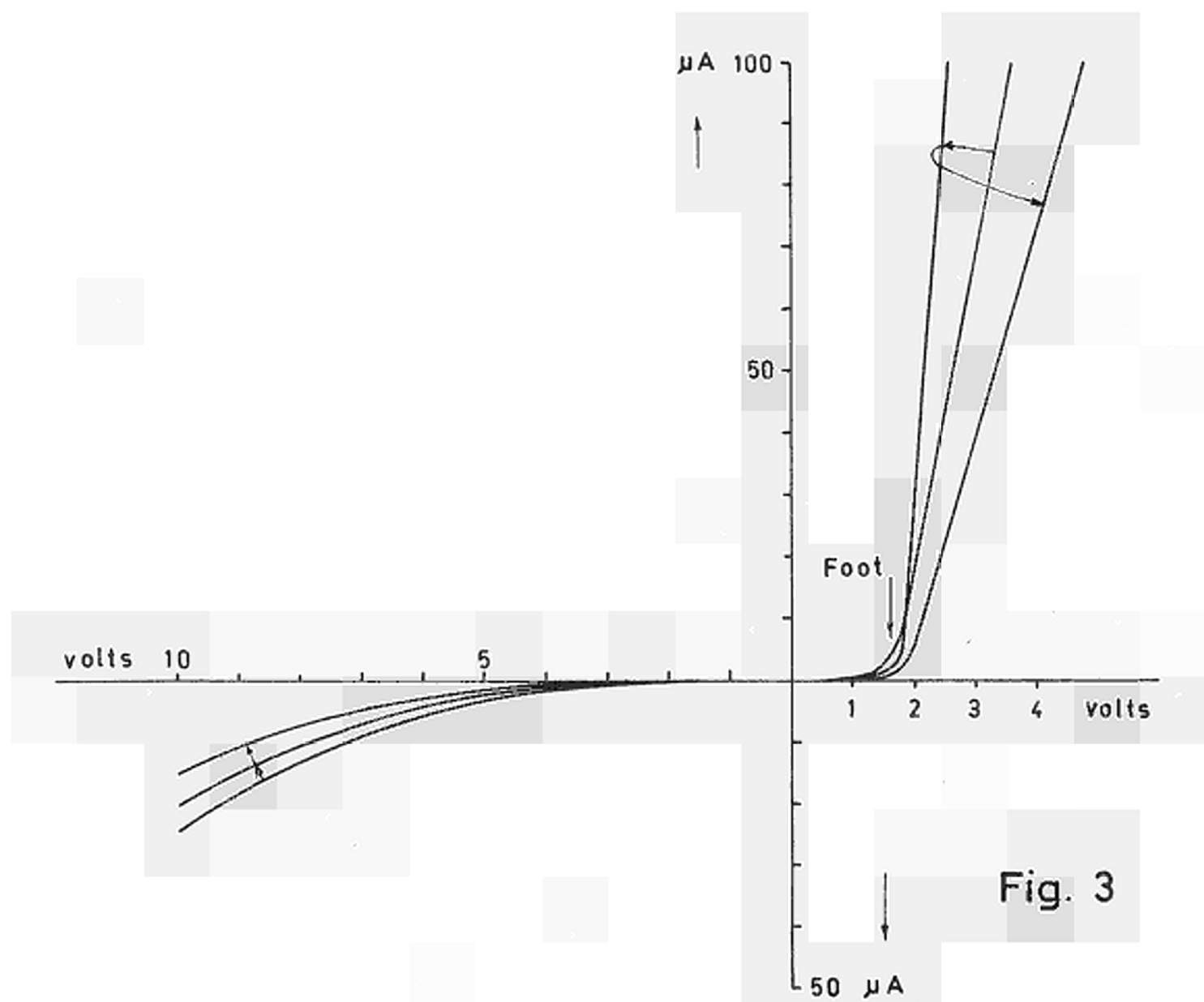
Schematic representation of the change of the forward and reverse characteristics of a SiC p-n junction upon reactor irradiation.

Change of the reverse current at a bias voltage of 0.9 volt and of the "foot" at a bias voltage of 0.8 volt.
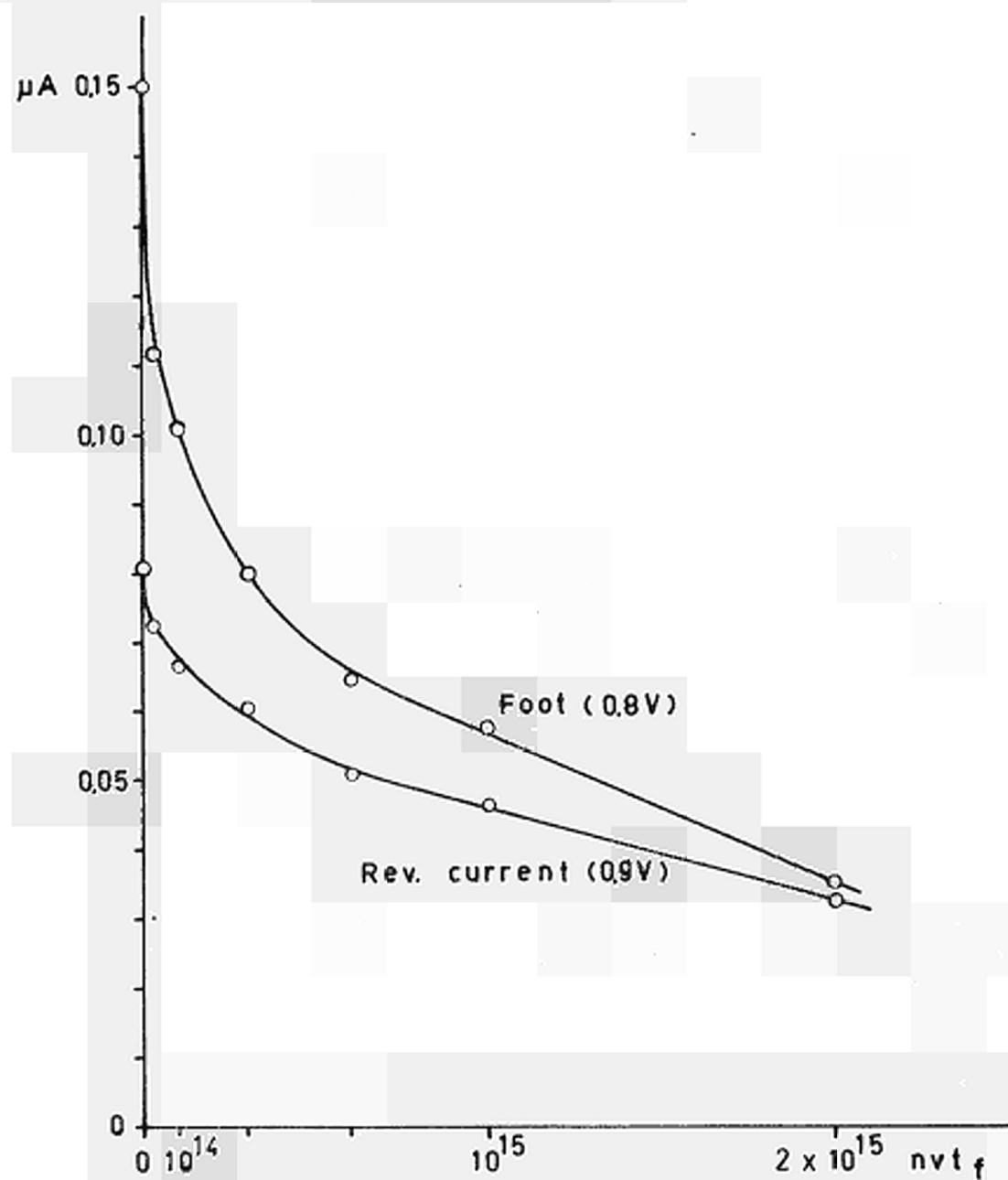
Fig. 4
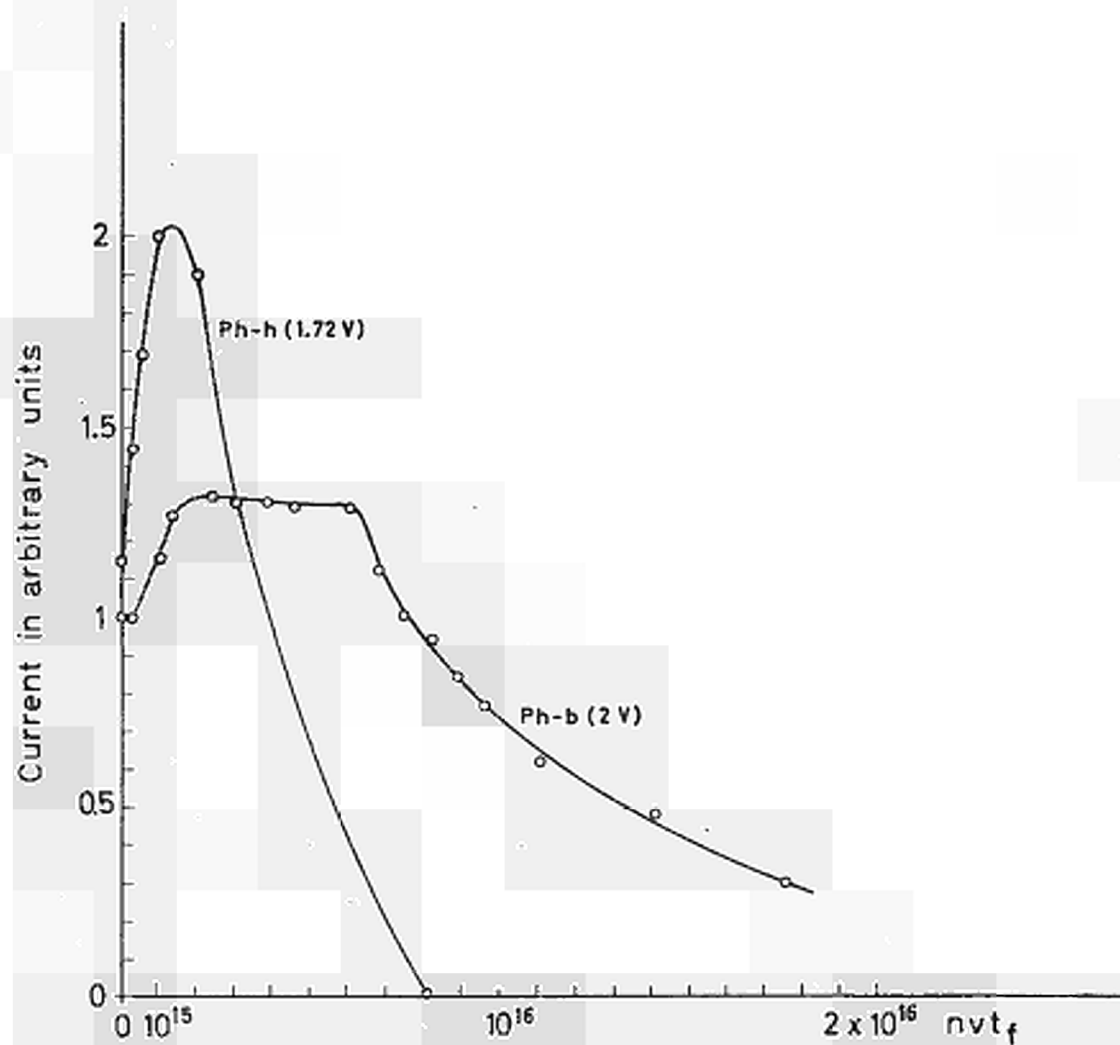
Fig. 5

Change of the forward current of junction Ph-h at a bias voltage of 1.7 volt and of junction Ph at a bias voltage of 2 volts.
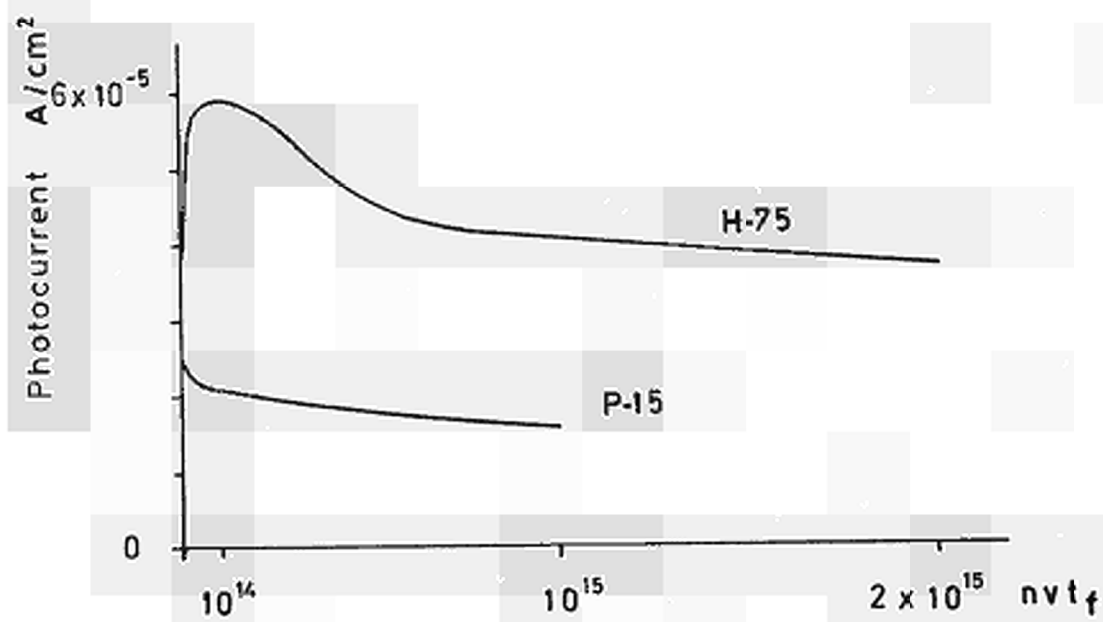
Fig. 6

Change of the short-circuit photocurrent upon reactor
irradiation of a sample junction of series H-75 and P-15.

	nvt$_f$	Slope
①	0	1.68 kt
②	1×10^{14}	1.06 kt
③	3×10^{14}	1.55 kt
④	6×10^{14}	1.59 kt
⑤	1×10^{15}	1.61 kt
⑥	2×10^{15}	1.66 kt
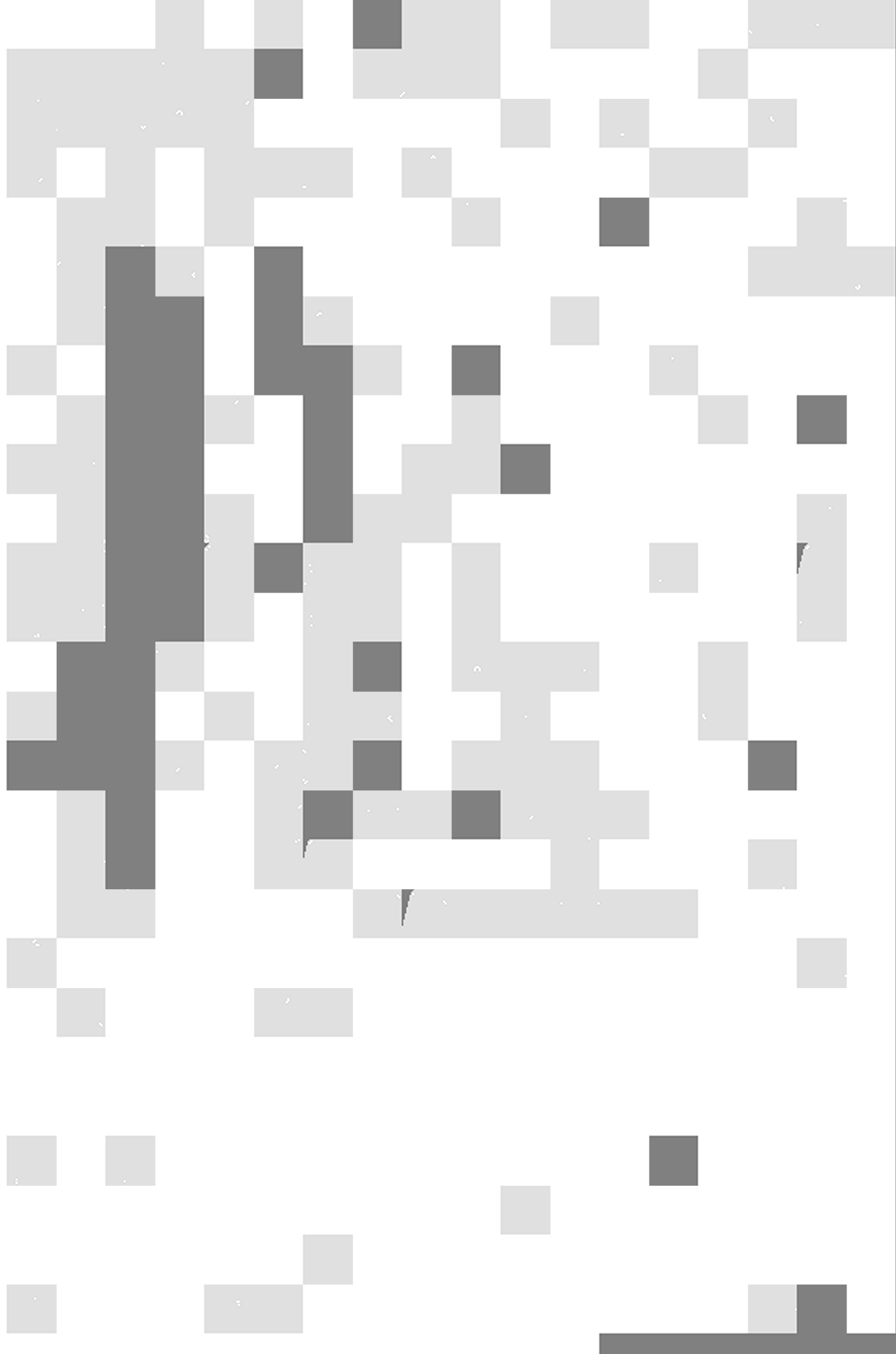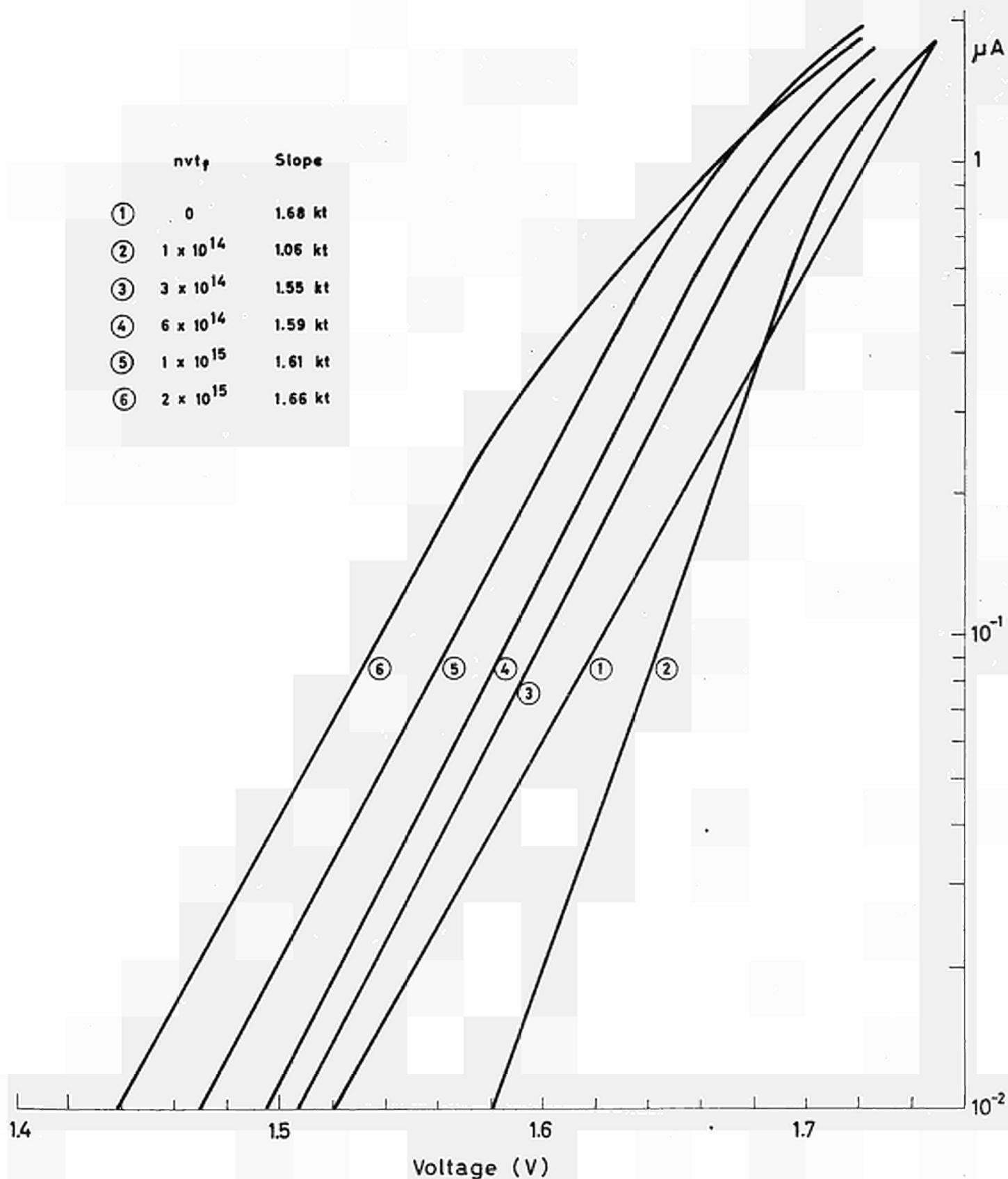
Voltage (V)

Fig. 7

ln I versus voltage curves of the forward characteristics ot junction Ph-h
at various doses of reactor irradiation obtained by subtracting the "foot„
from the original characteristics.
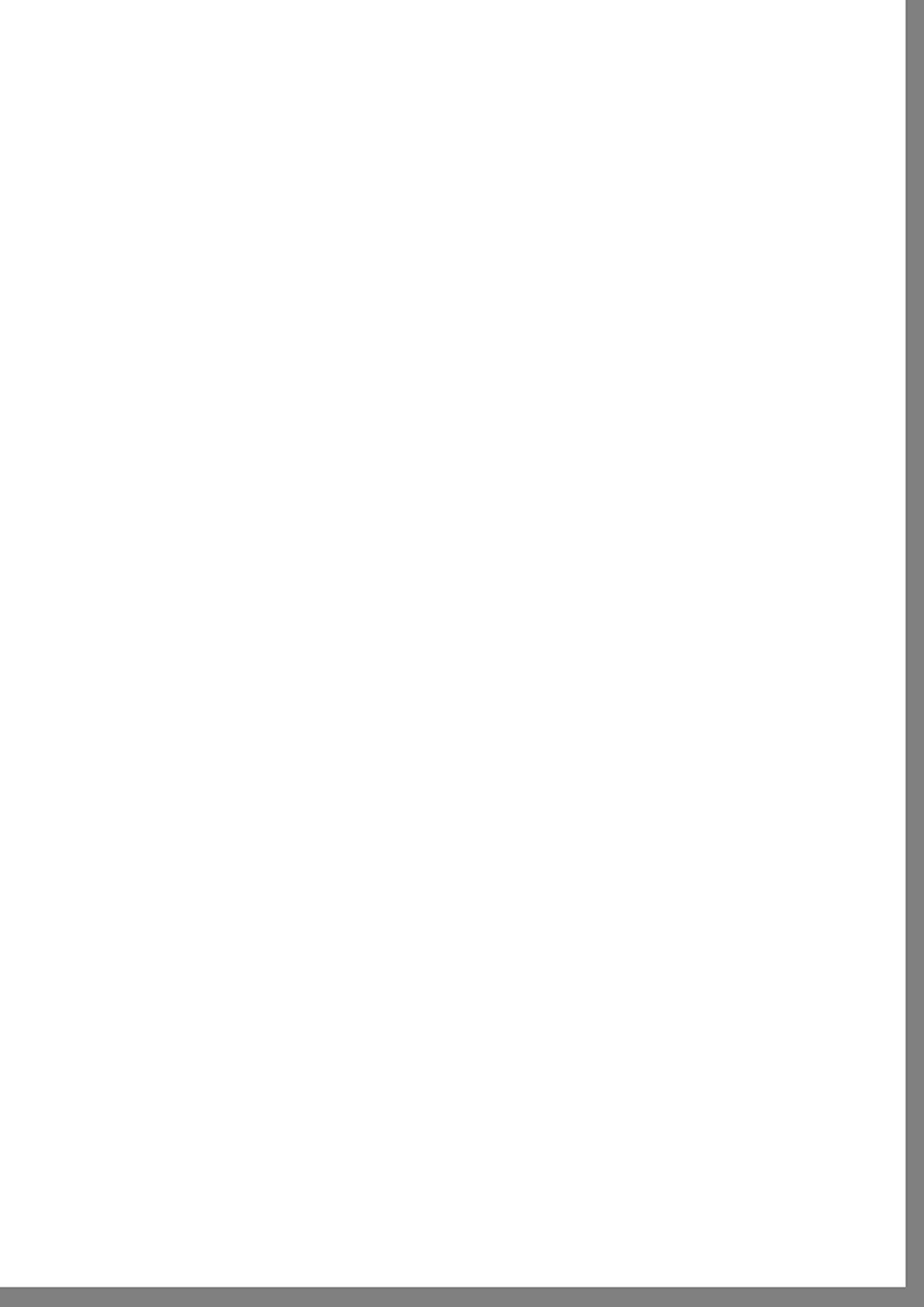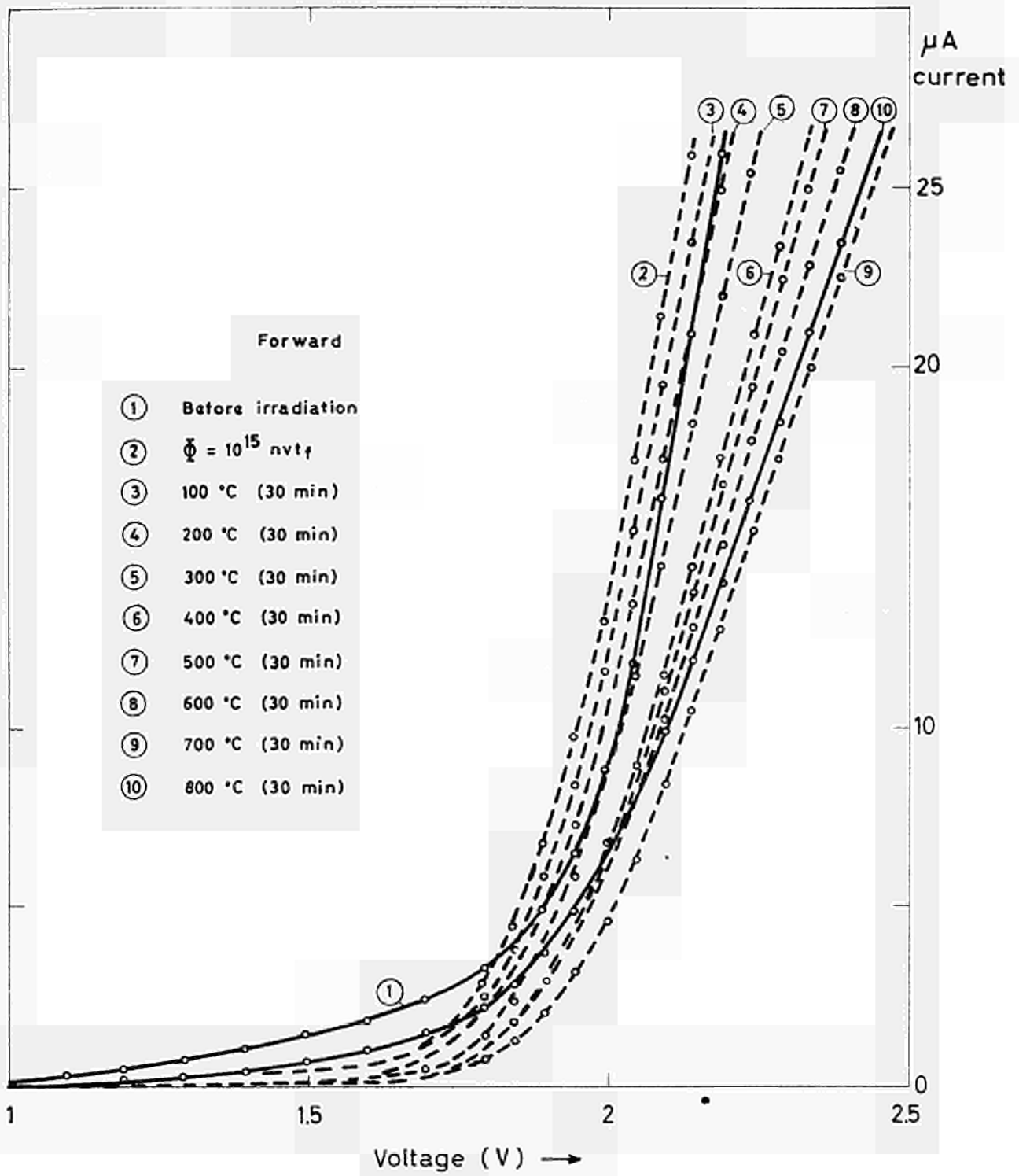
Fig. 8

Change of forward characteristic upon pulse annealing.

μA
current

Reverse

① Before irradiation

② $\bar{\Phi} = 10^{15}$ nvt_f

③ 100 °C (30 min)

④ 200 °C (30 min)

⑤ 300 °C (30 min)

⑥ 400 °C (30 min)

⑦ 500 °C (30 min)

⑧ 600 °C (30 min)

⑨ 700 °C (30 min)

⑩ 800 °C (30 min)
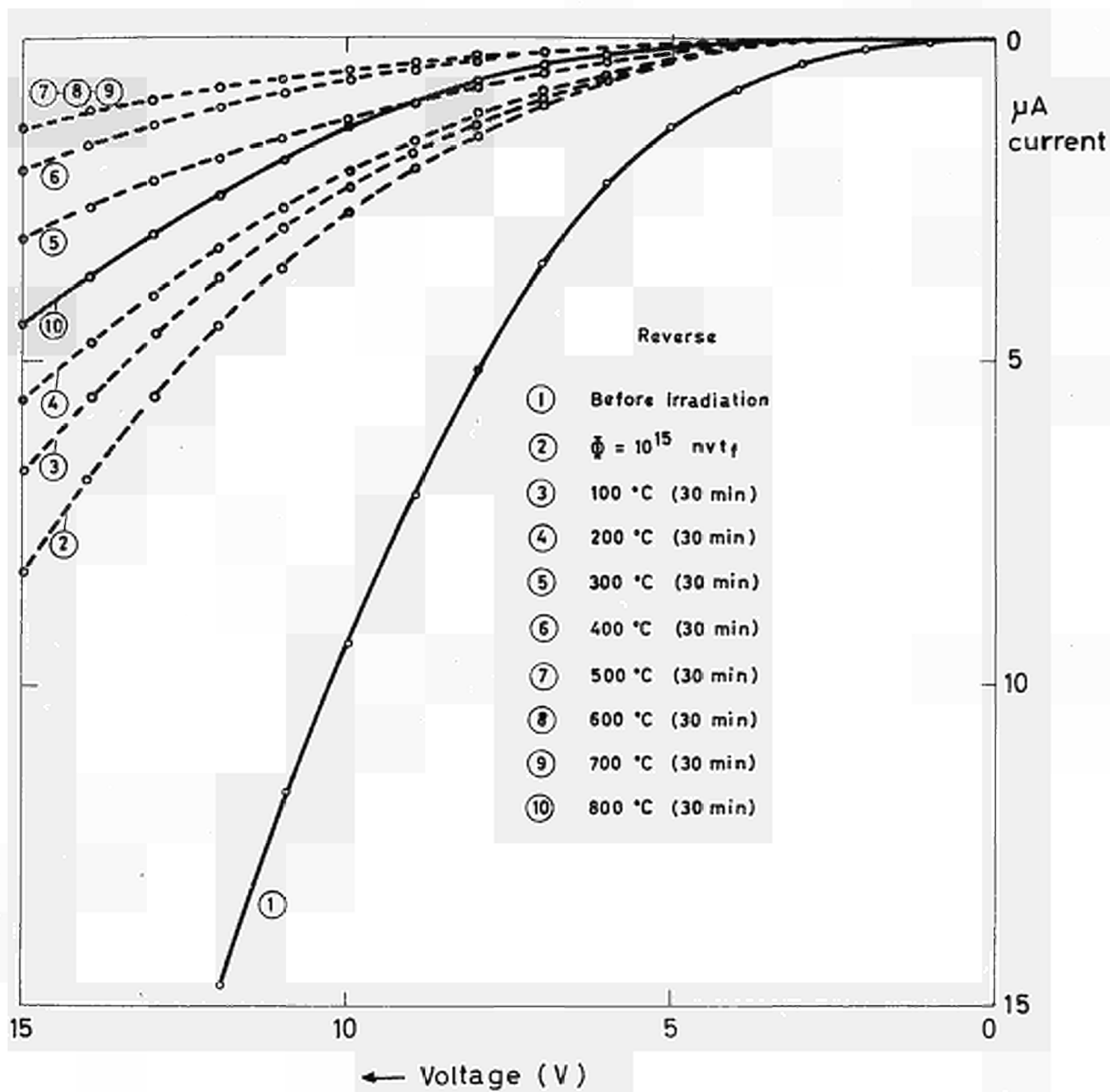
← Voltage (V)

Fig. 9

Change of reverse characteristic upon pulse annealing
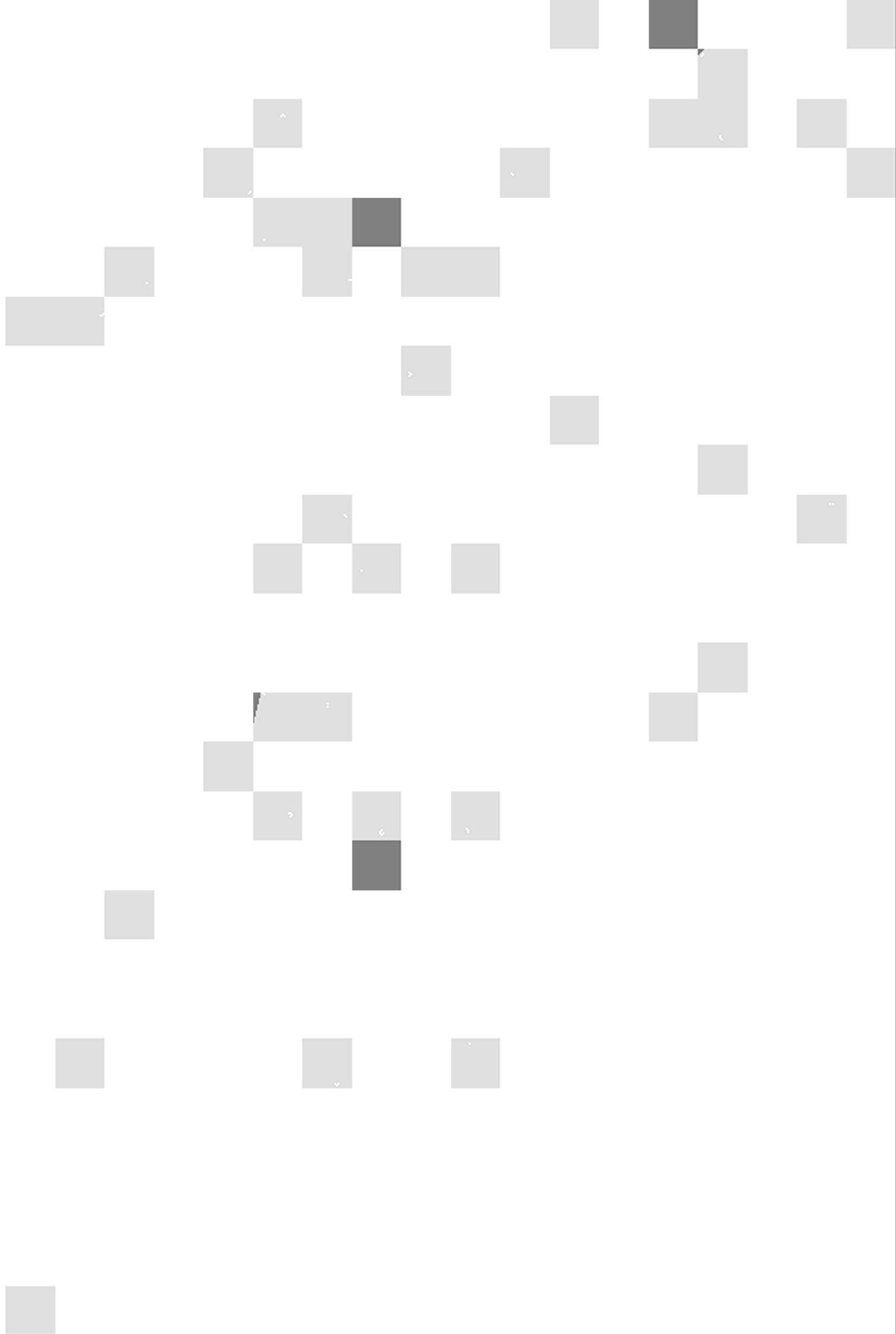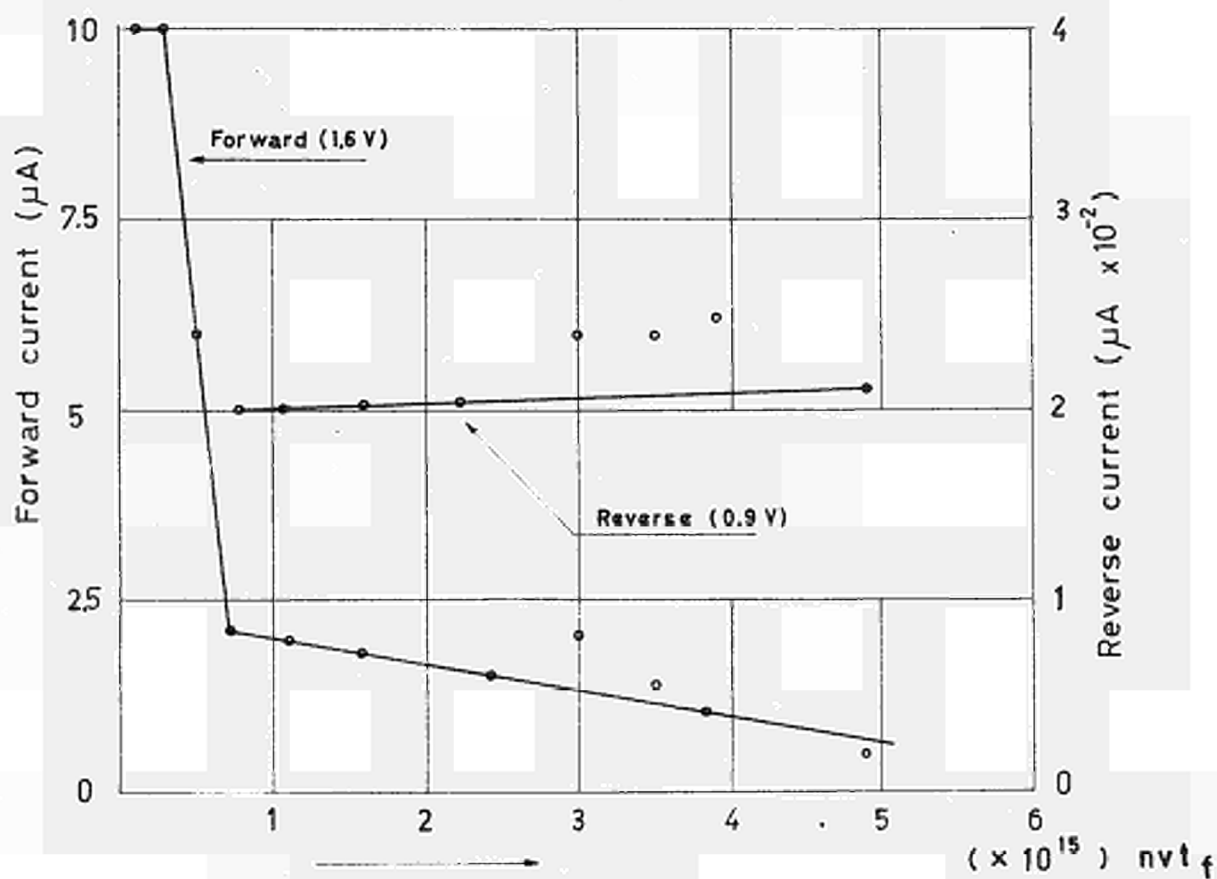
Fig. 10

Change of the forward and the reverse current at a constant bias voltage of a grown SiC diode during reactor irradiation at a temperature of 500 °C.
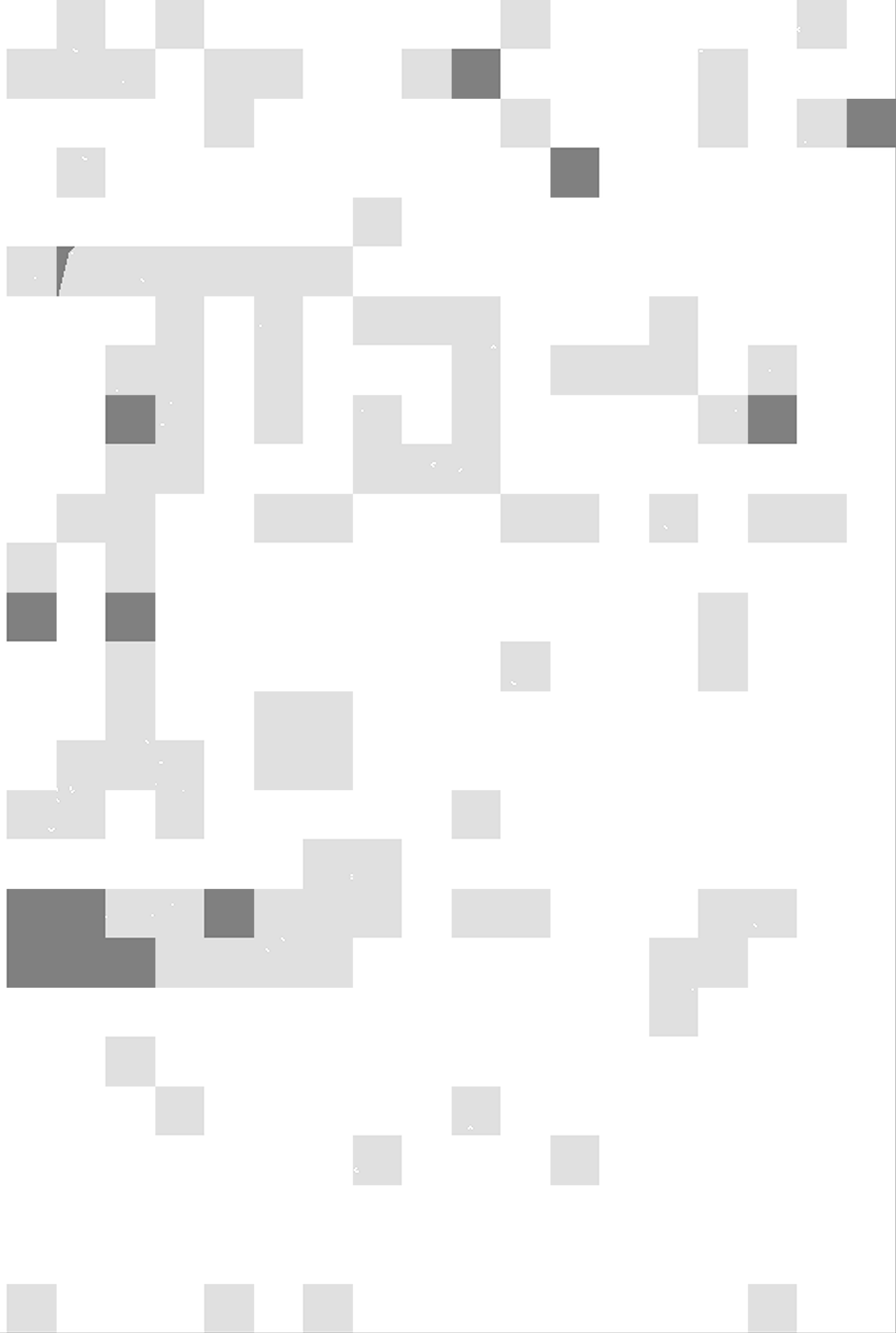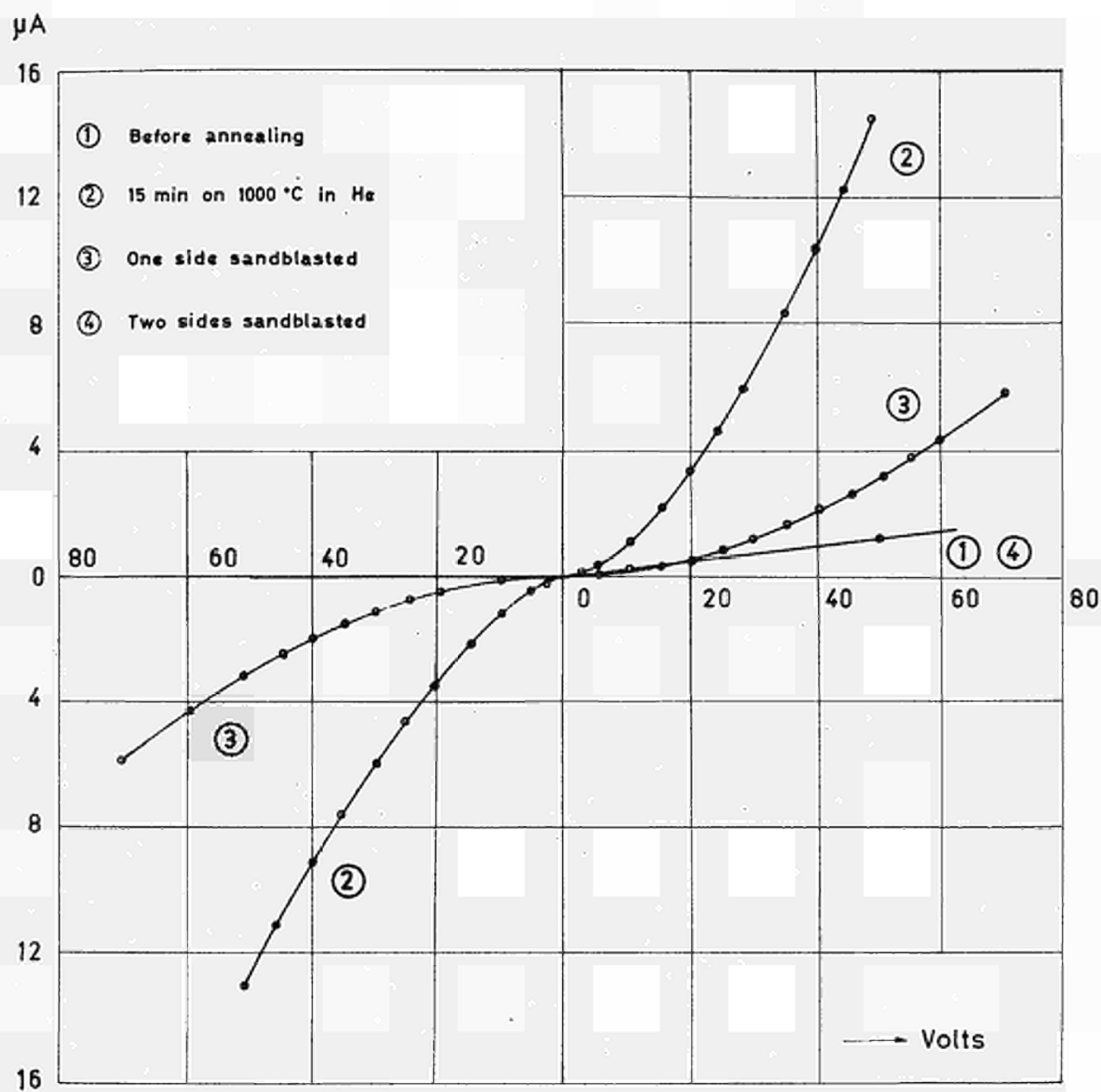
Fig. 11

Surface conduction after heat treatment at 1000 °C.
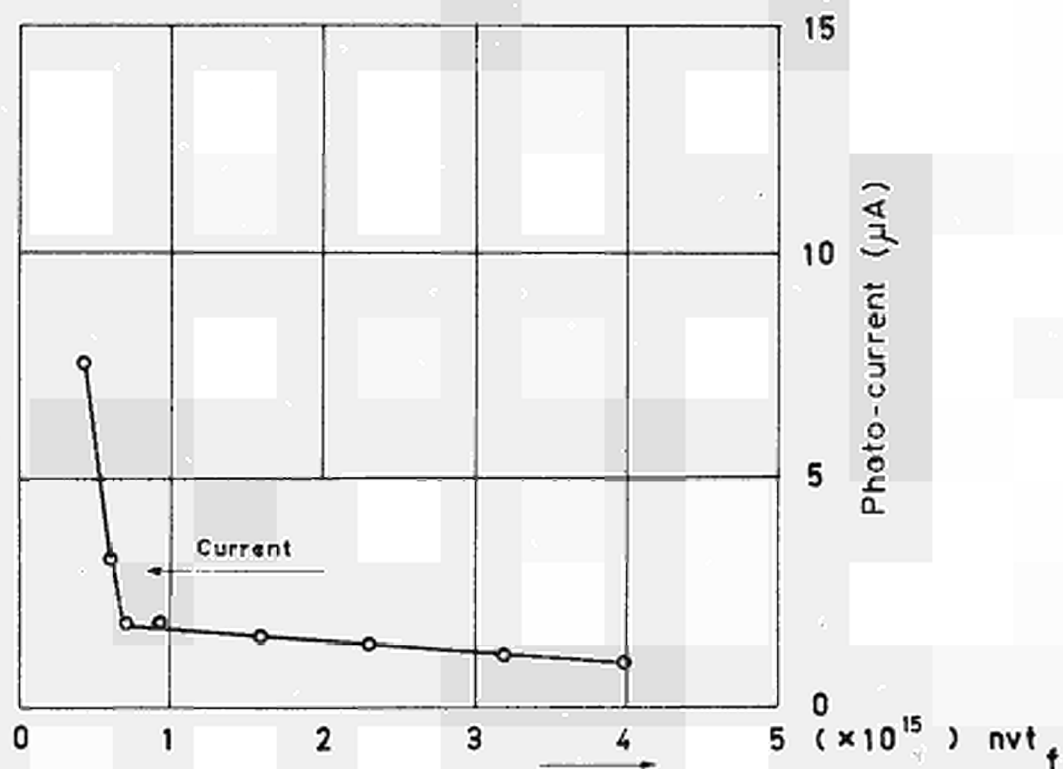
Fig. 12

Change of photocurrent of a grown SiC diode at 500 °C
during reactor irradiation.
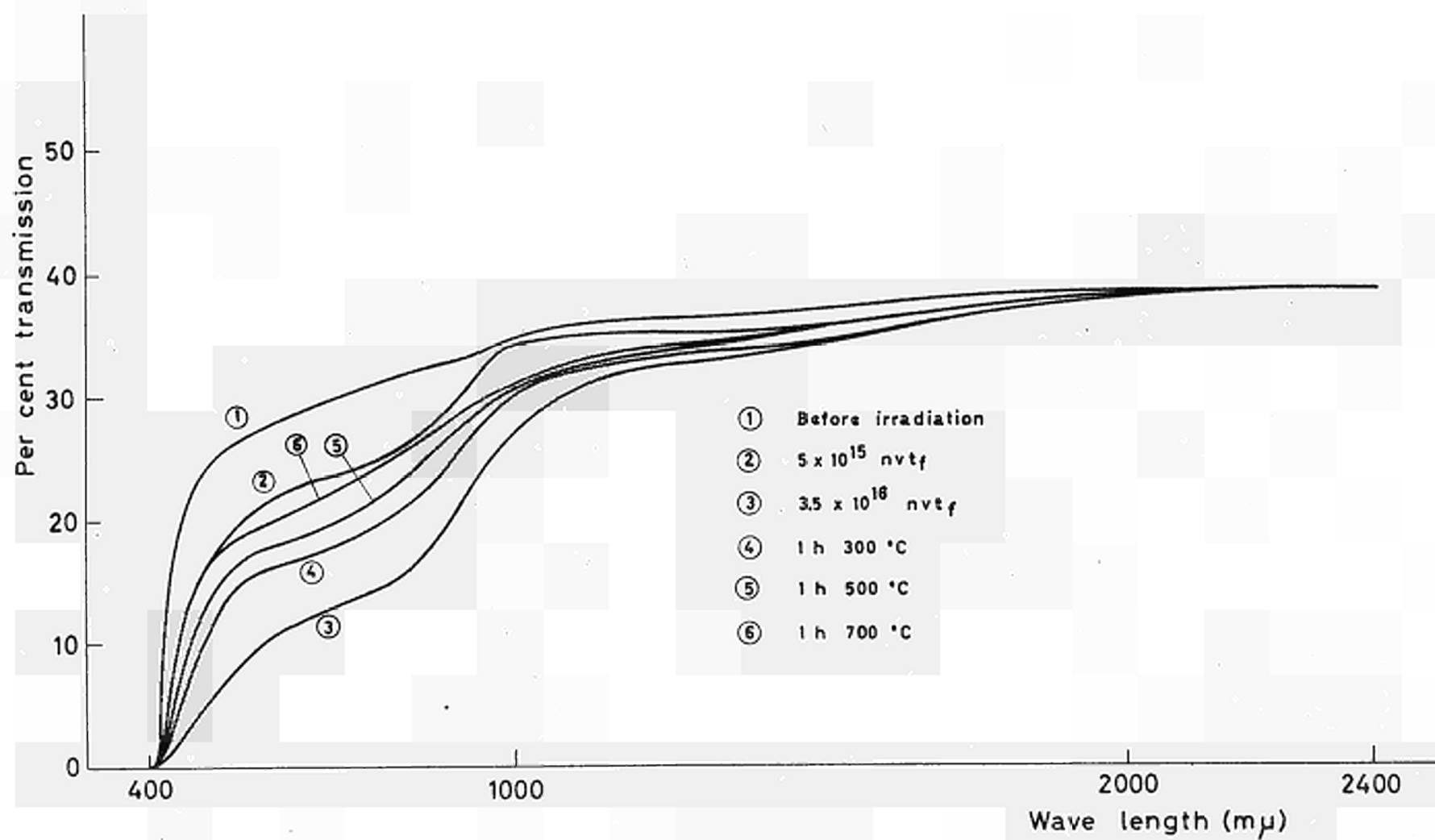
Fig. 13

Change of transmission of a SiC single crystal upon reactor irradiation and subsequent annealing.

Legend (as shown in figure):
- ① Before irradiation
- ② 5×10^{15} nvt$_f$
- ③ 3.5×10^{16} nvt$_f$
- ④ 1 h 300 °C
- ⑤ 1 h 500 °C
- ⑥ 1 h 700 °C

Axes: Per cent transmission (vertical), Wave length (mμ) (horizontal)
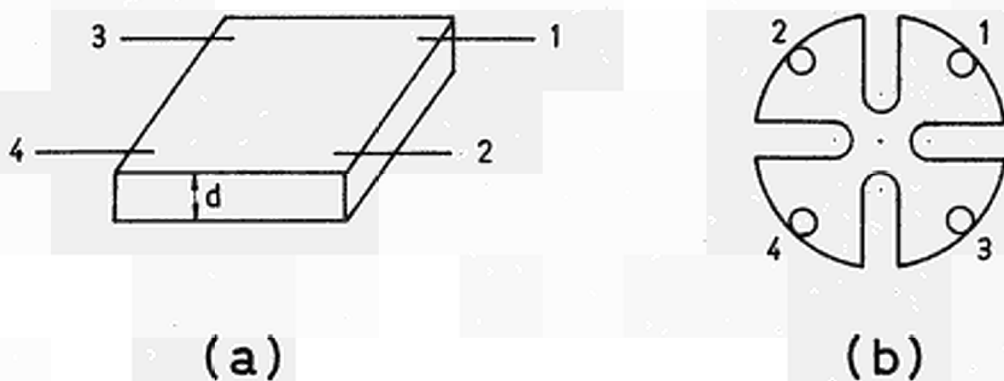
Fig.14

Arrangement of probes for resistivity and Hall measurements
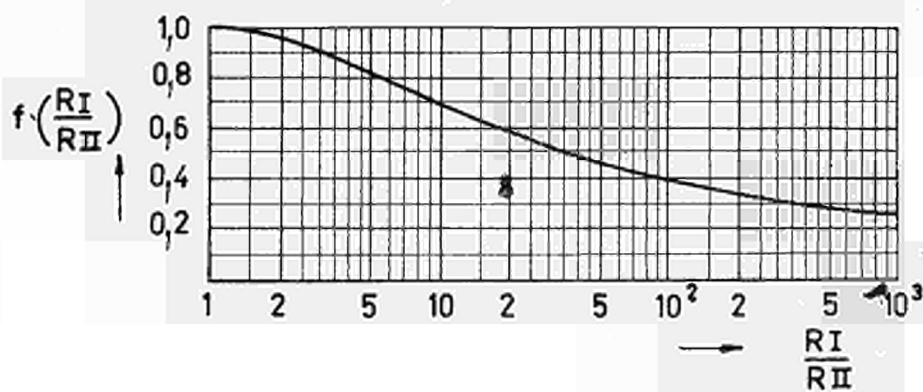
Fig. 15

The function $f\left(\dfrac{RI}{RII}\right)$ used for determining the specific resistivity.

C/349/6
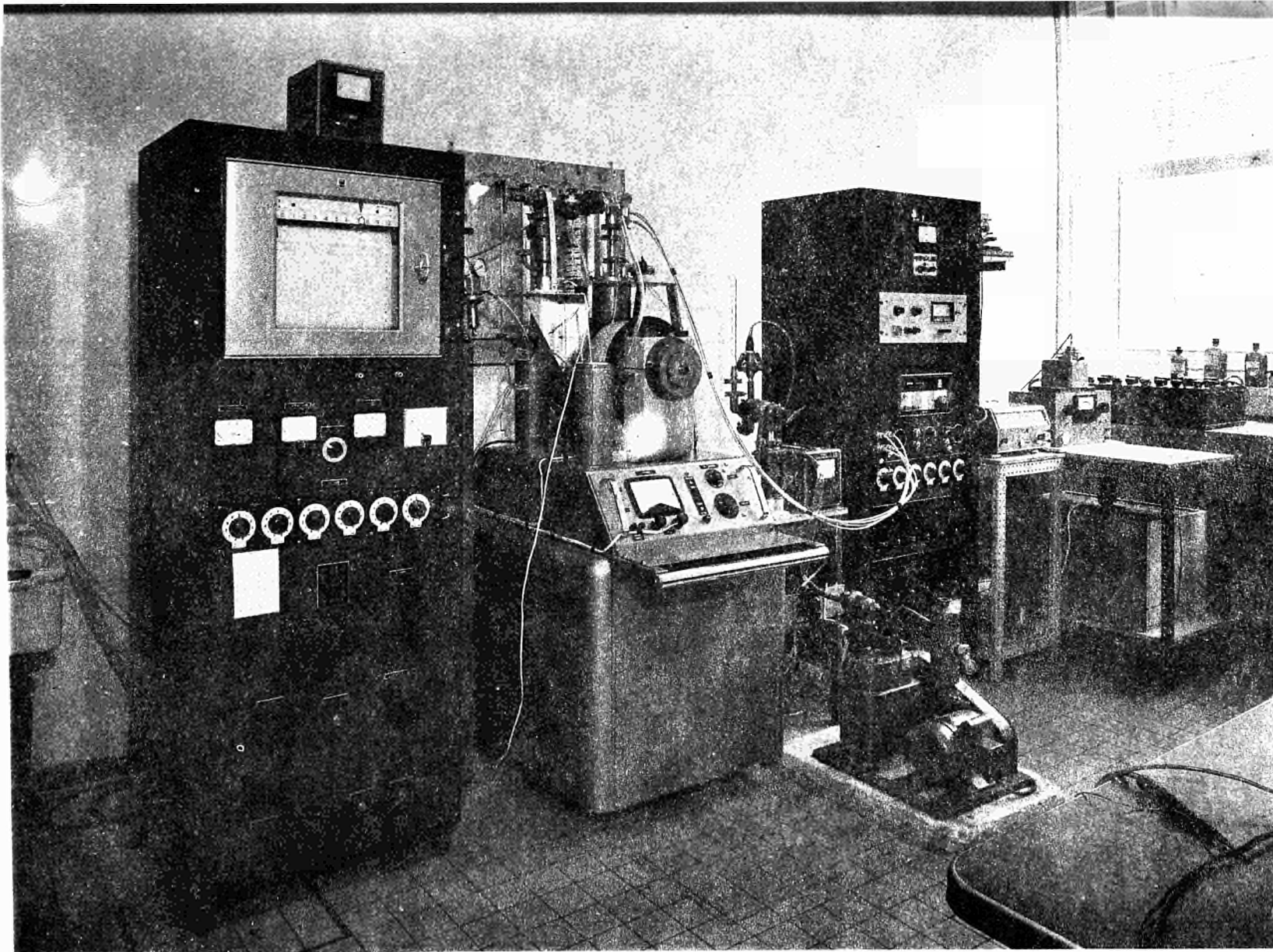
Fig.16

Apparatus for the Hall and resistivity measurements.
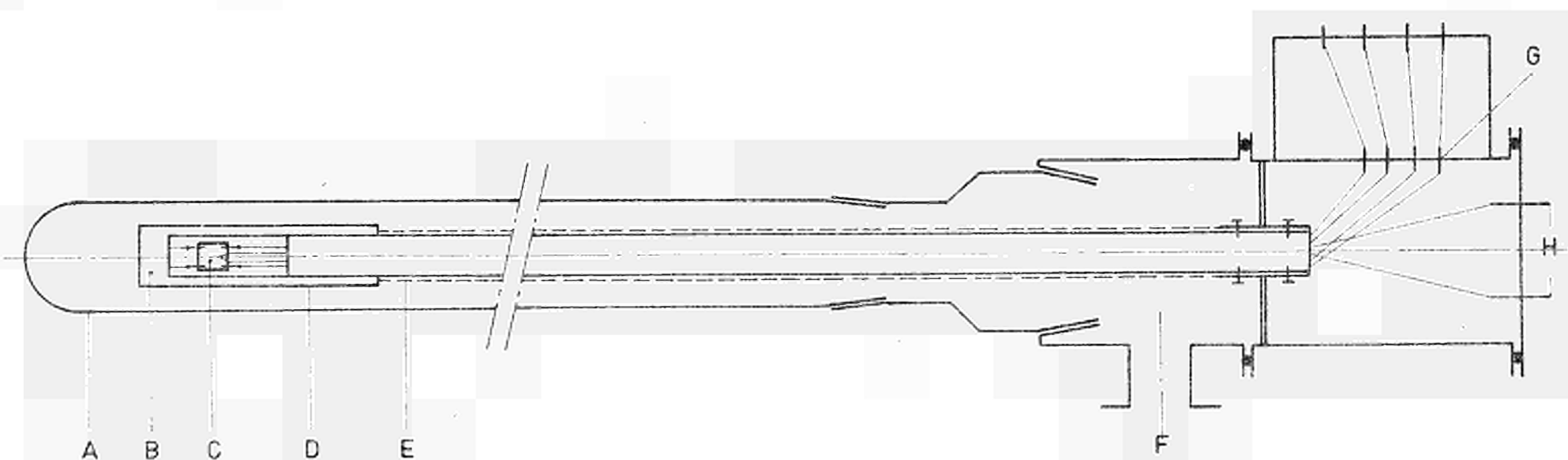
A   Alumina tube
B   Alumina tube with 6 channels
C   Crystal
D   Tantalum cylinder
E   Copper shielding
F   Vacuum connection and Argon inlet
G   Metal-glass seals with contact wires
H   Metal-glass seals with thermocouple wires

Fig. 17

Specimen holder for high temperature.
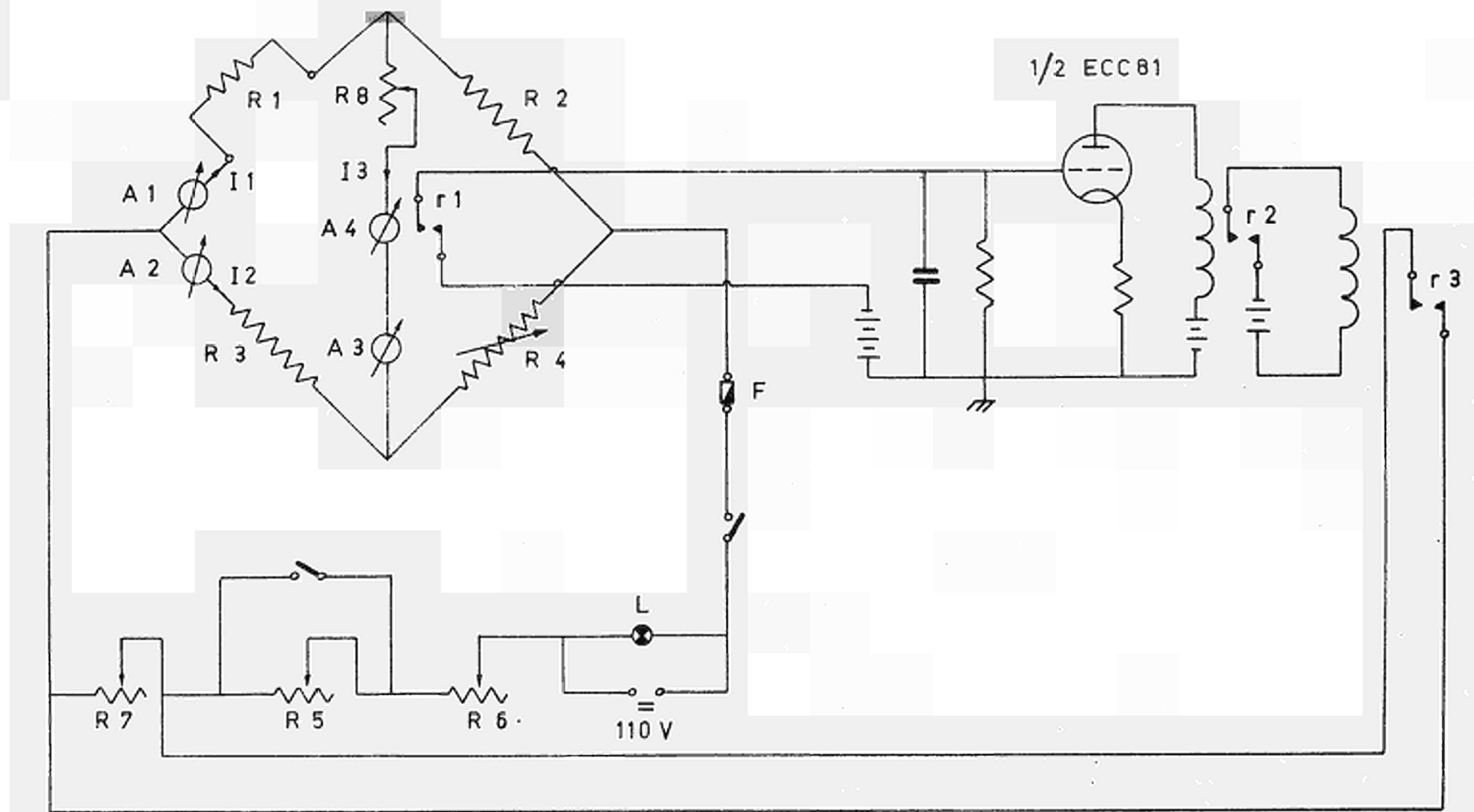
R 1	Oven resistance	R 7	50 ohm 630 W
R 2	5 ohm	R 8	50 kohm
R 3	5 kohm	A 1	Ammeter 6 A
R 4	$0.1 - 10^5$ ohm	A 2	Ammeter 25 mA
R 5	250 ohm 630 W	A 3	Ammeter 100 µA
R 6	20 ohm 630 W	A 4	Contact Ammeter 1 mA

Fig. 18

Circuit of the oven regulator.
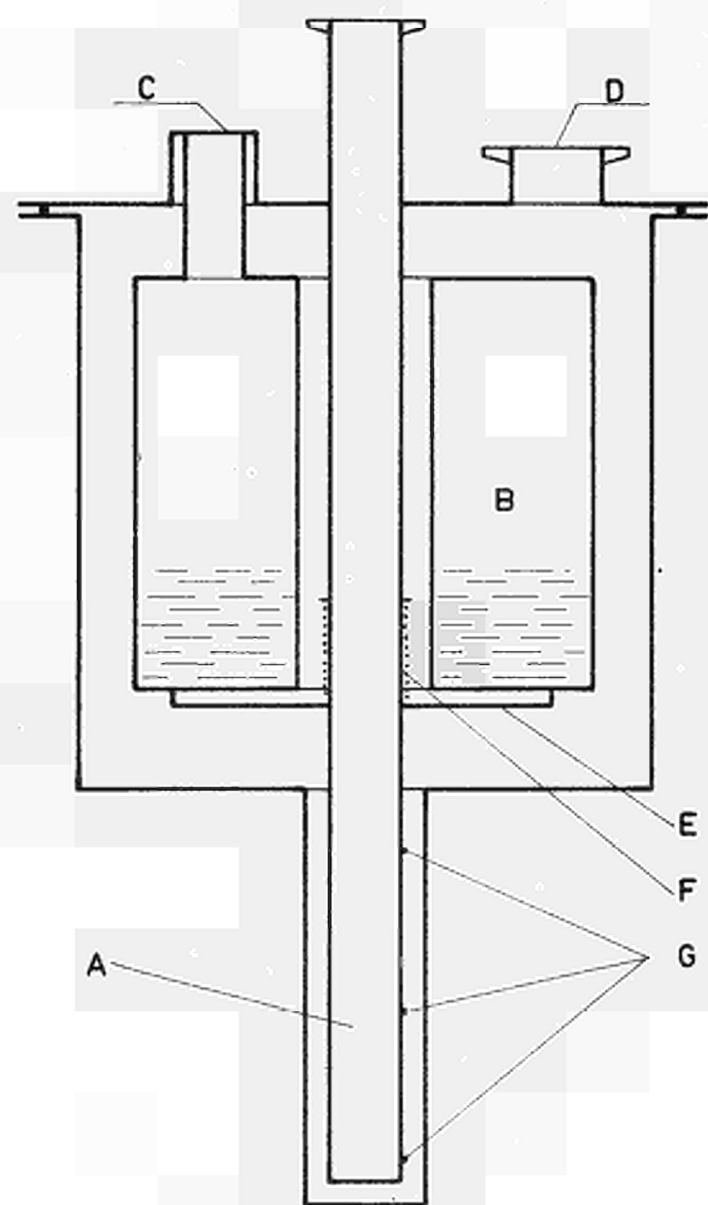
A	Measuring chamber
B	Liquid nitrogen
C	Filling tube
D	To vacuum system
E	Thermal shunt
F	Heater winding
G	Thermocouples

Fig. 19

Cryostat of all-metal construction.

Fig. 20

Conductivity of p-type Si C vs 1/T

C / 349 / 63

Fig. 21

Hole concentration of p-type SiC vs 1/T.

Fig. 22

Hole concentration multiplied by $(10^3/T)^{3/2}$ vs $1/T$.

C/349/63
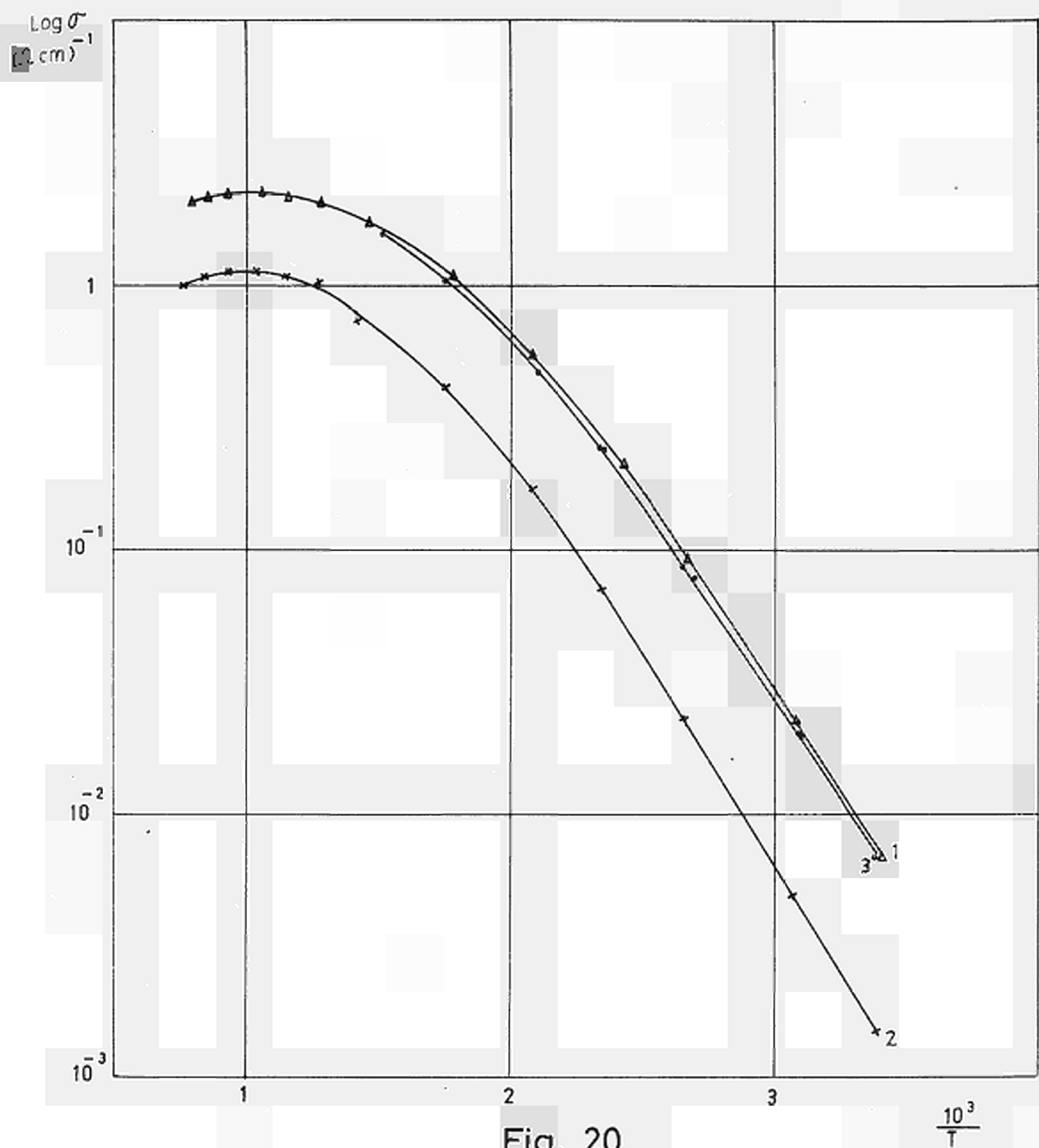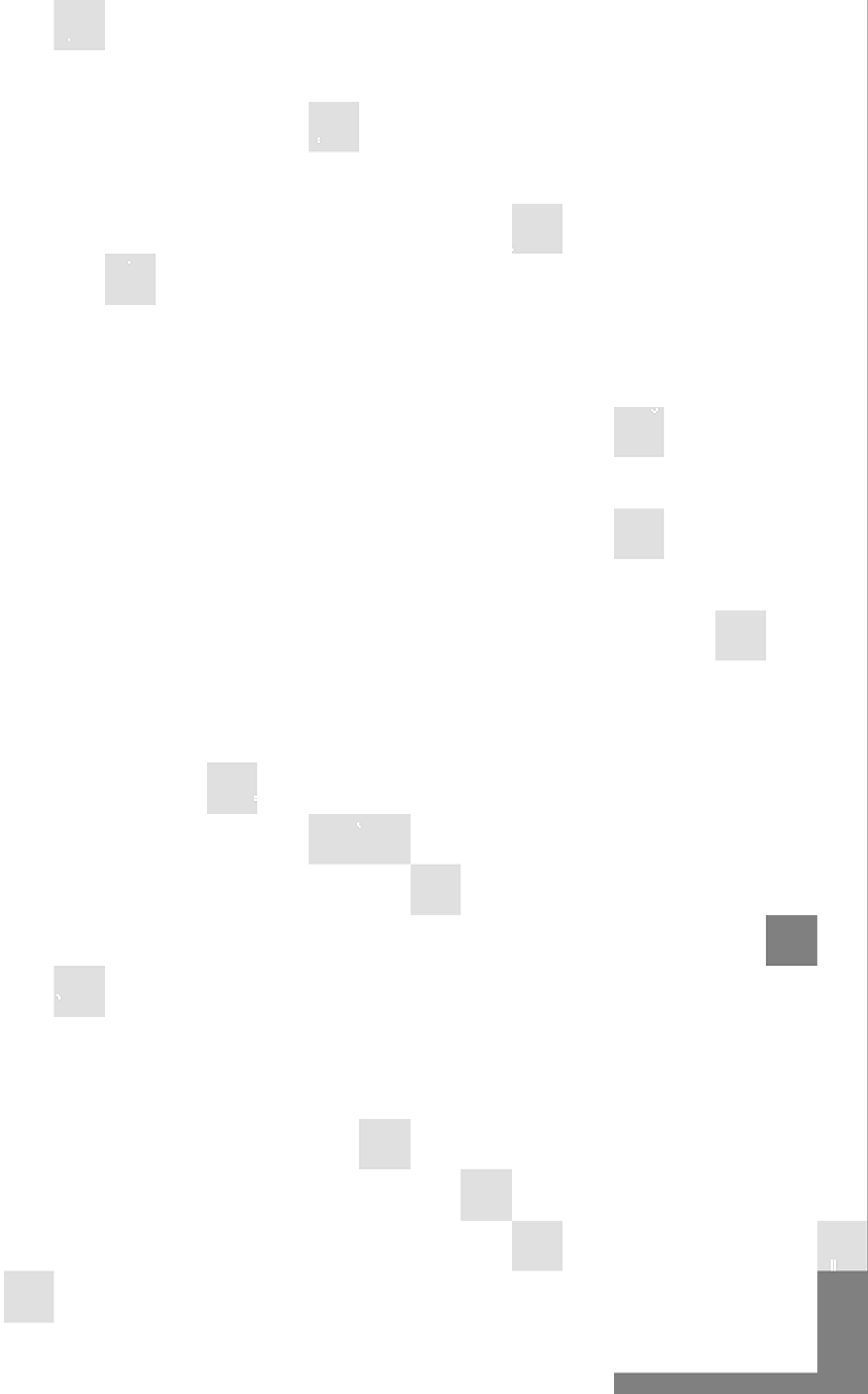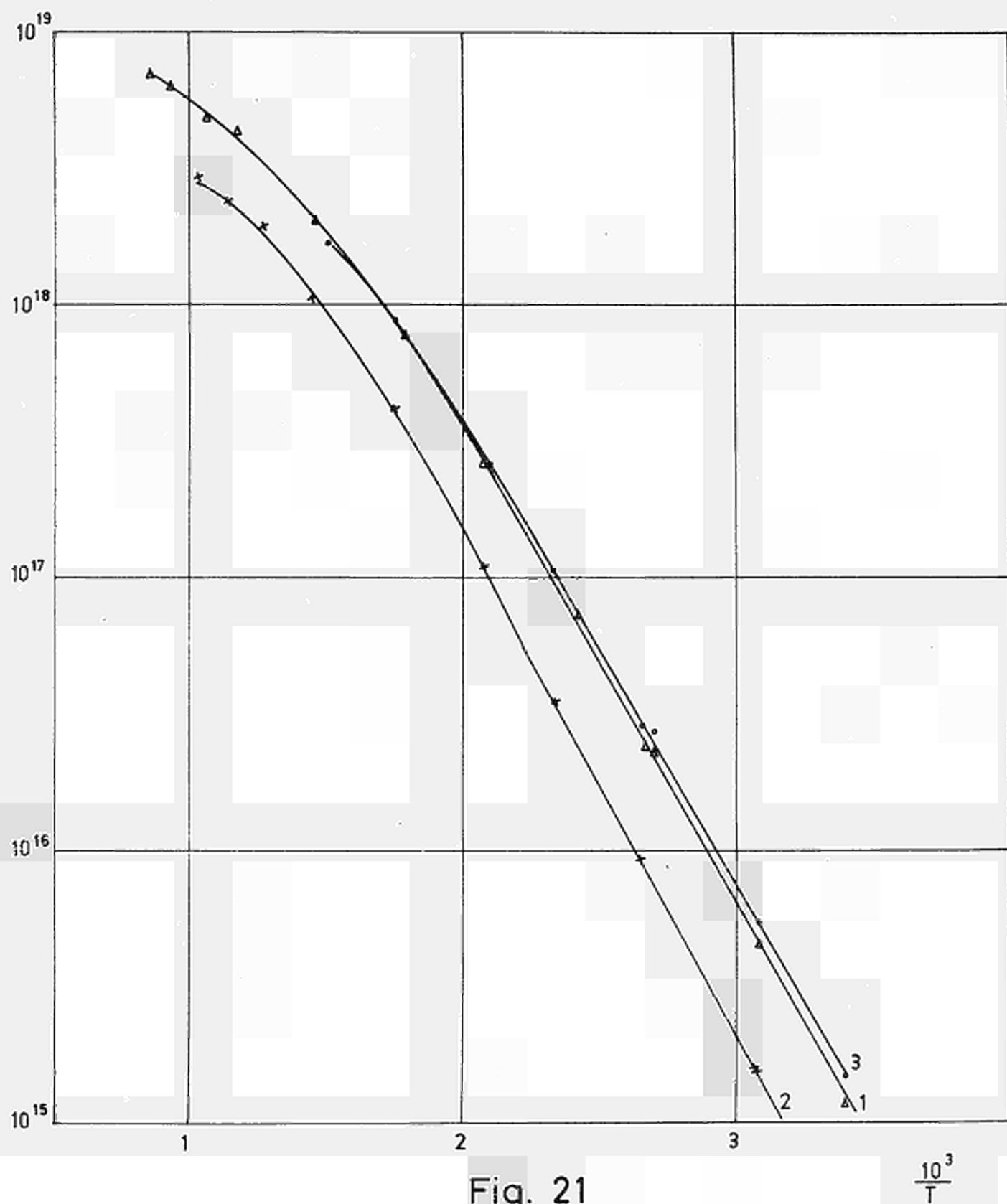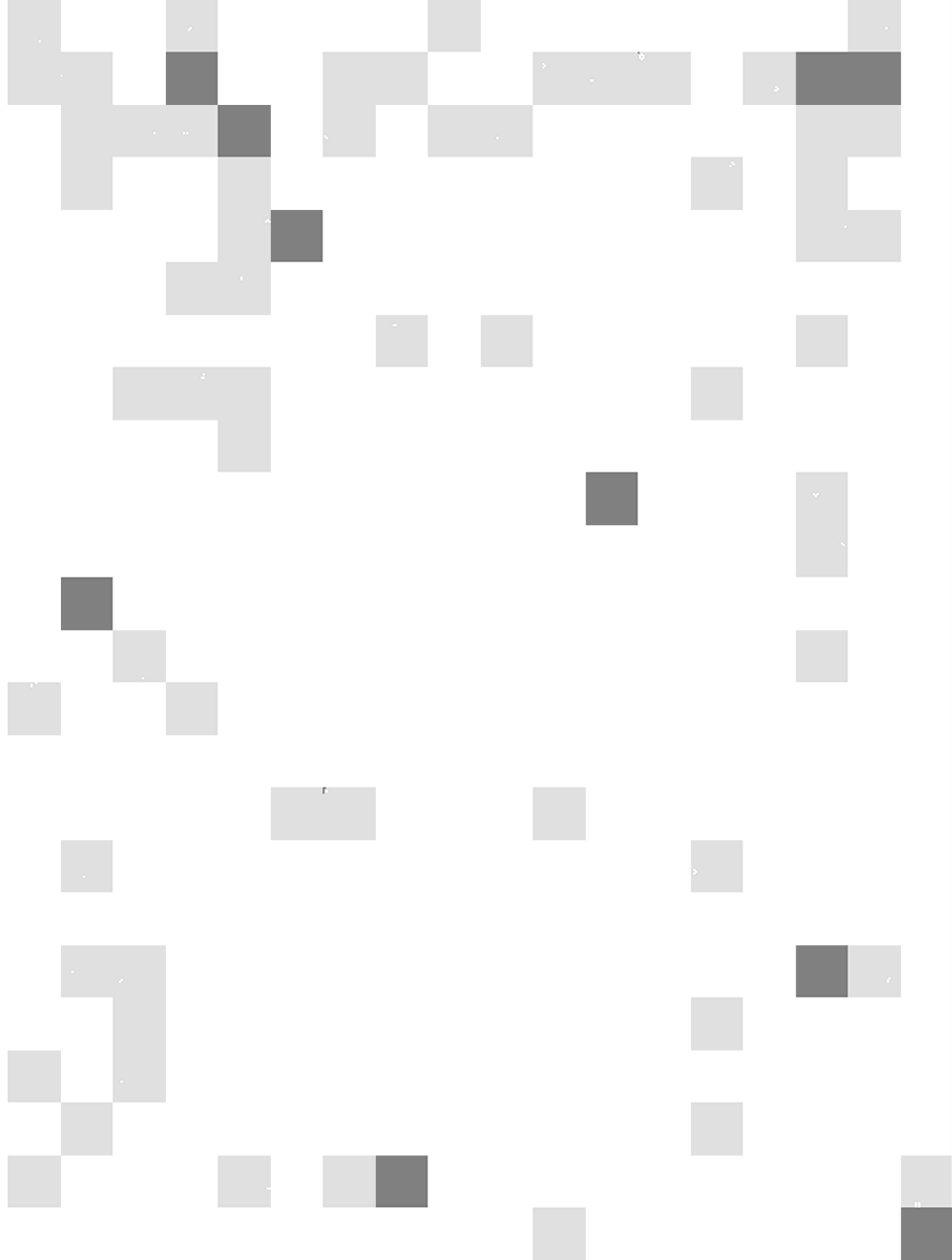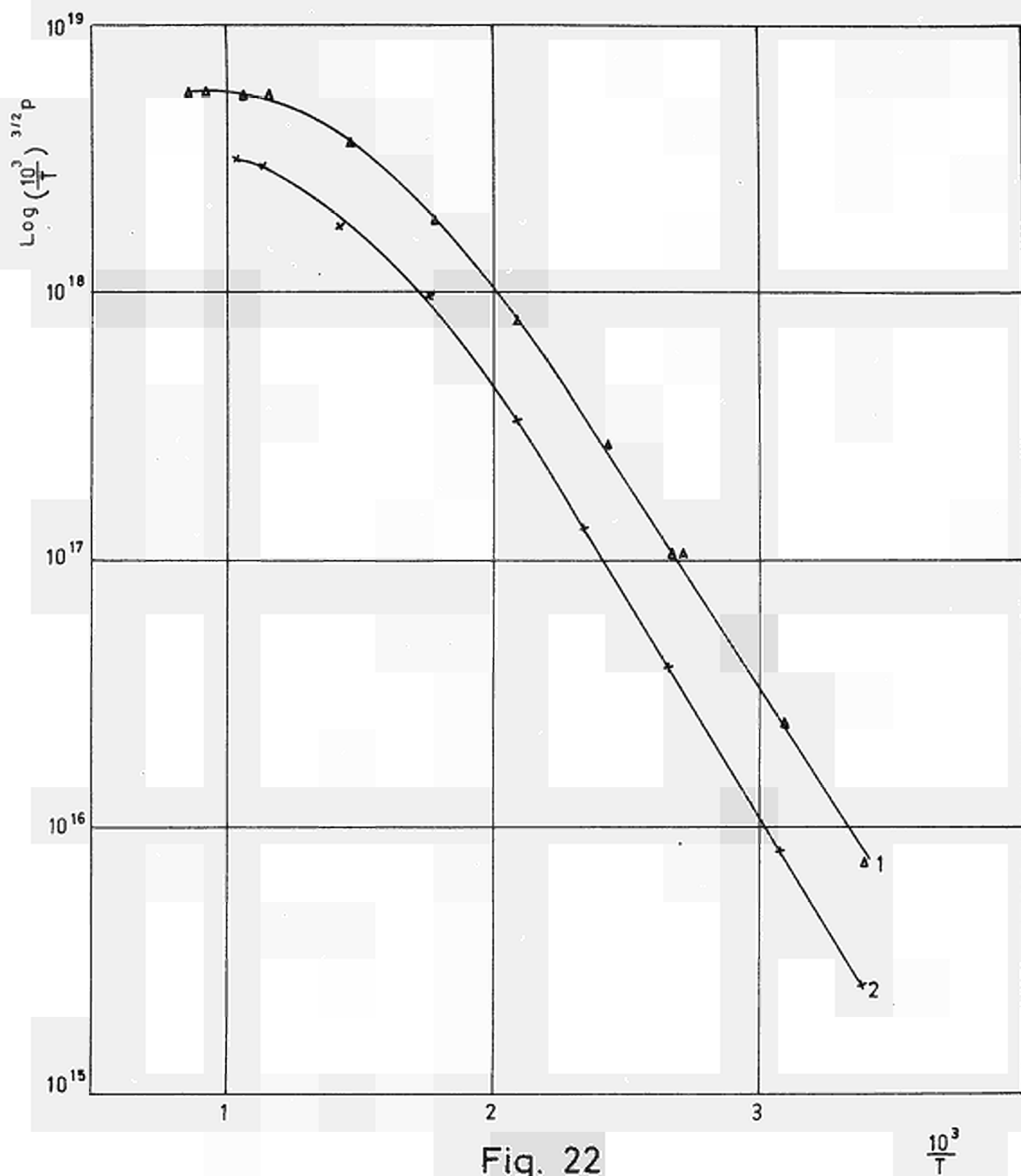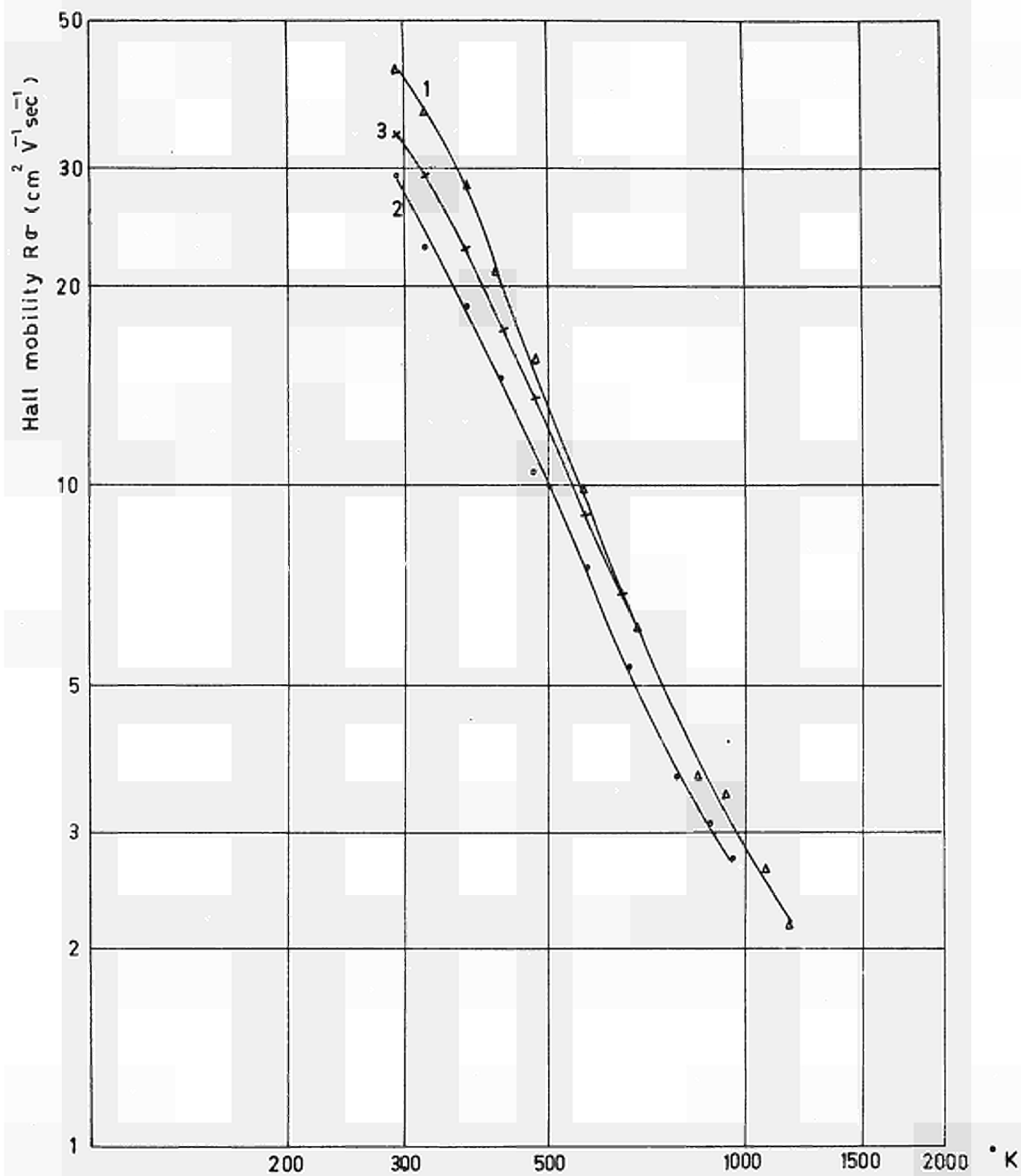
Fig. 23

Hall mobility of p-type SiC vs T
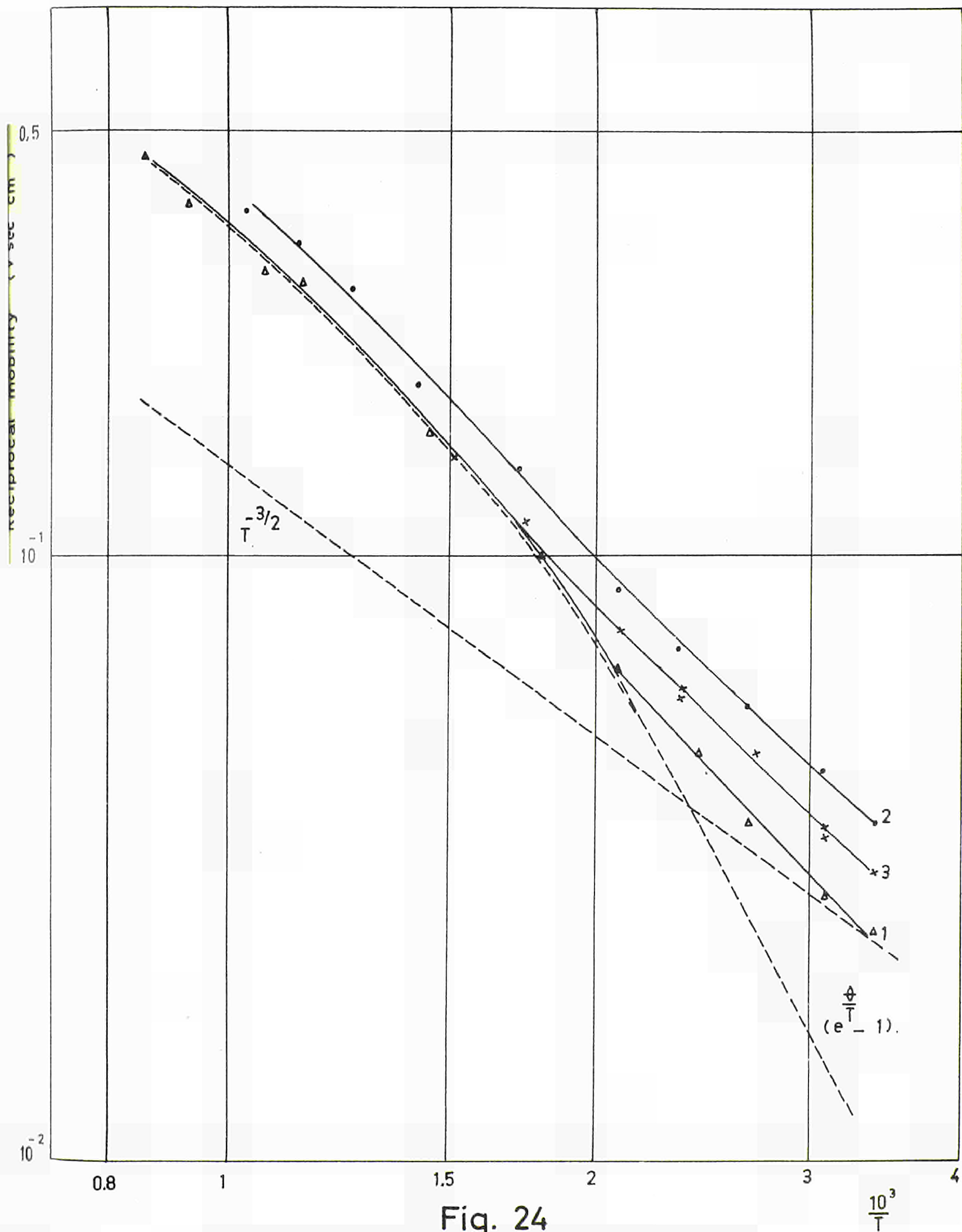
Fig. 24

Reciprocal Hall mobility of p-type SiC vs 1/T.

1349/63
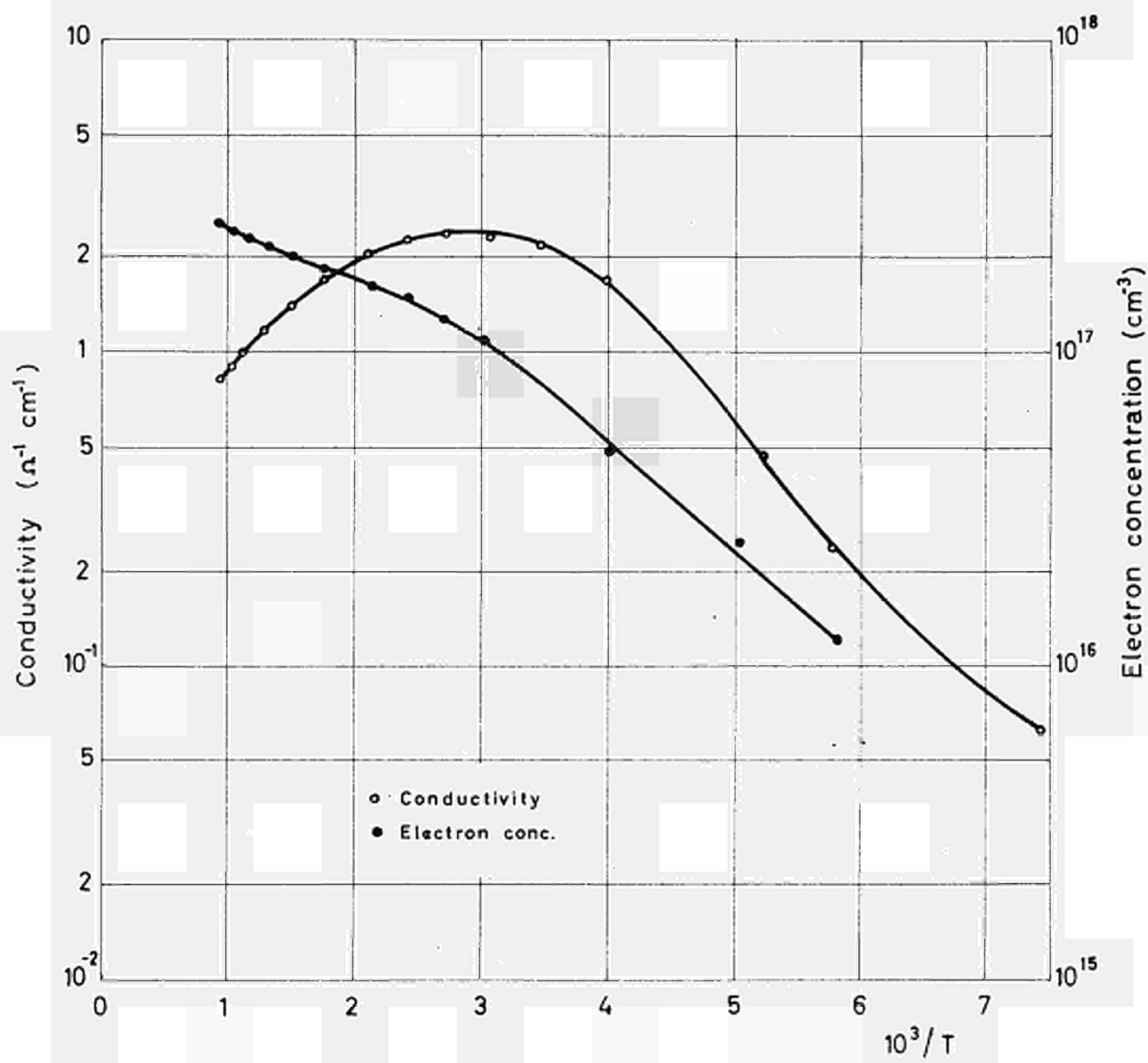
Fig. 25

Conductivity and electron concentration of n-type SiC vs 1/T
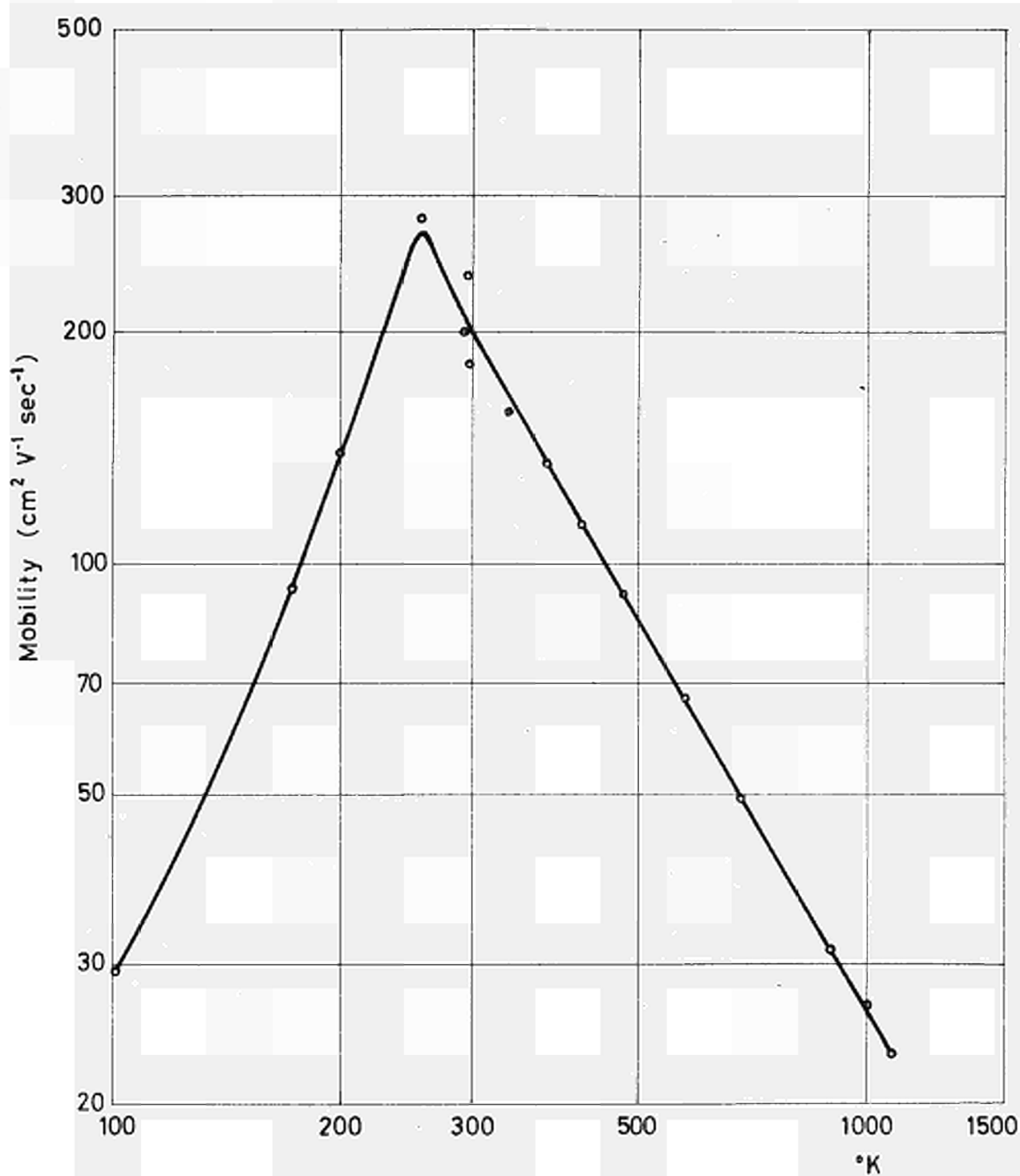
Fig. 26

Hall mobility of n-type SiC vs

Fig. 27

II/53   Conductivity of n-type SiC as a function of temperature before and after irradiation
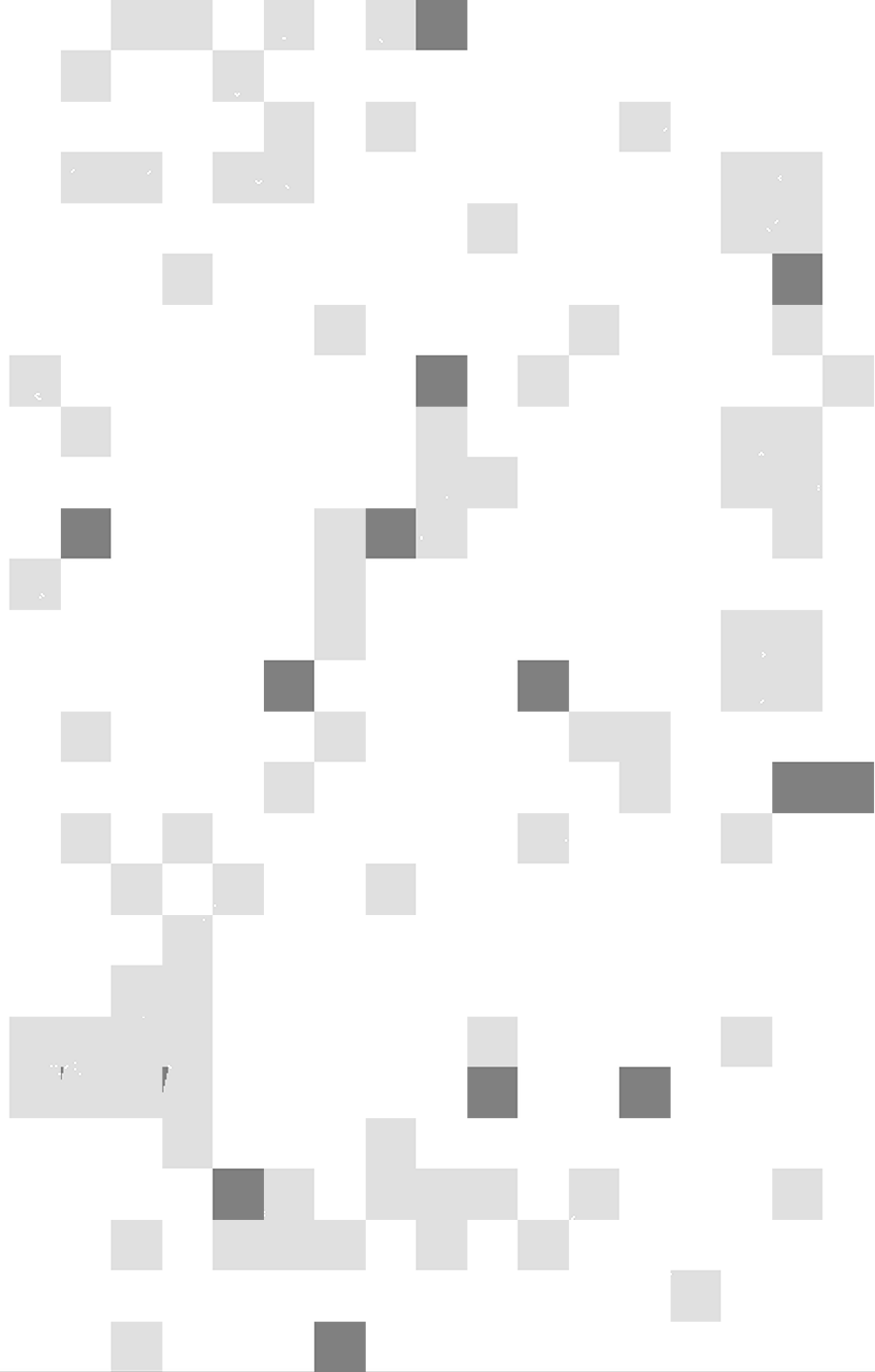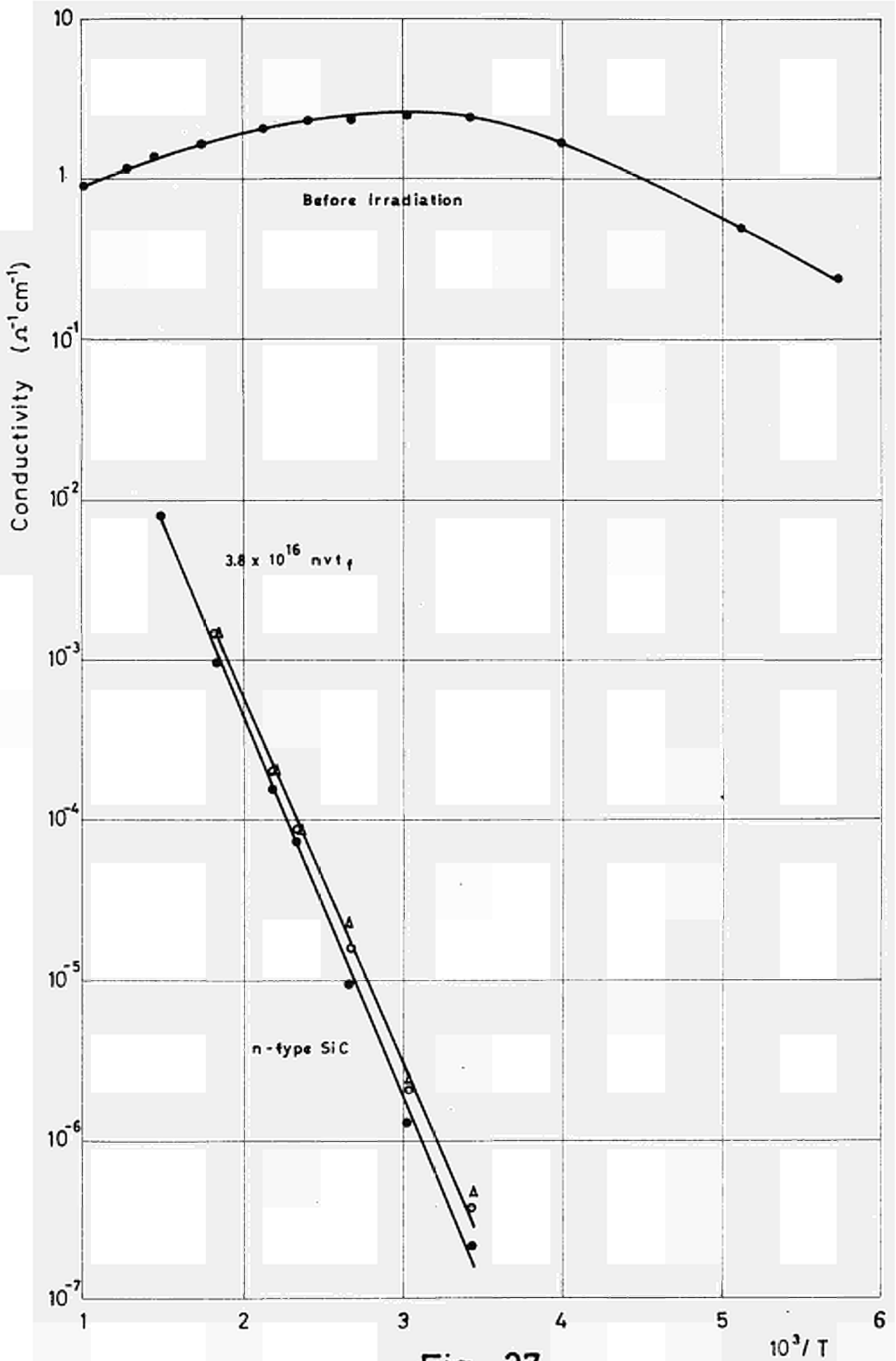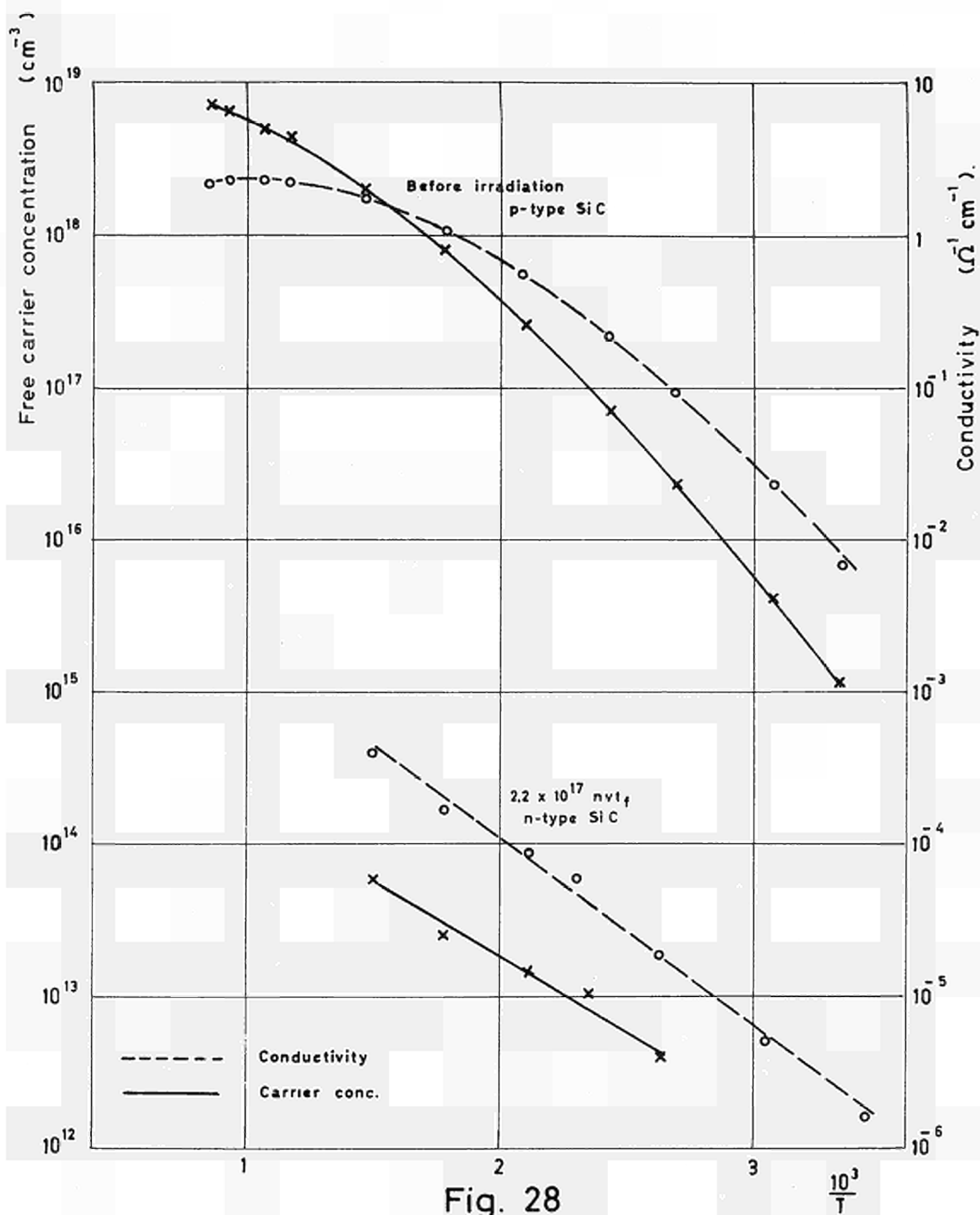
Fig. 28

Conductivity and carrier concentration of p-type SiC as a
function of temperature before and after irradiation.
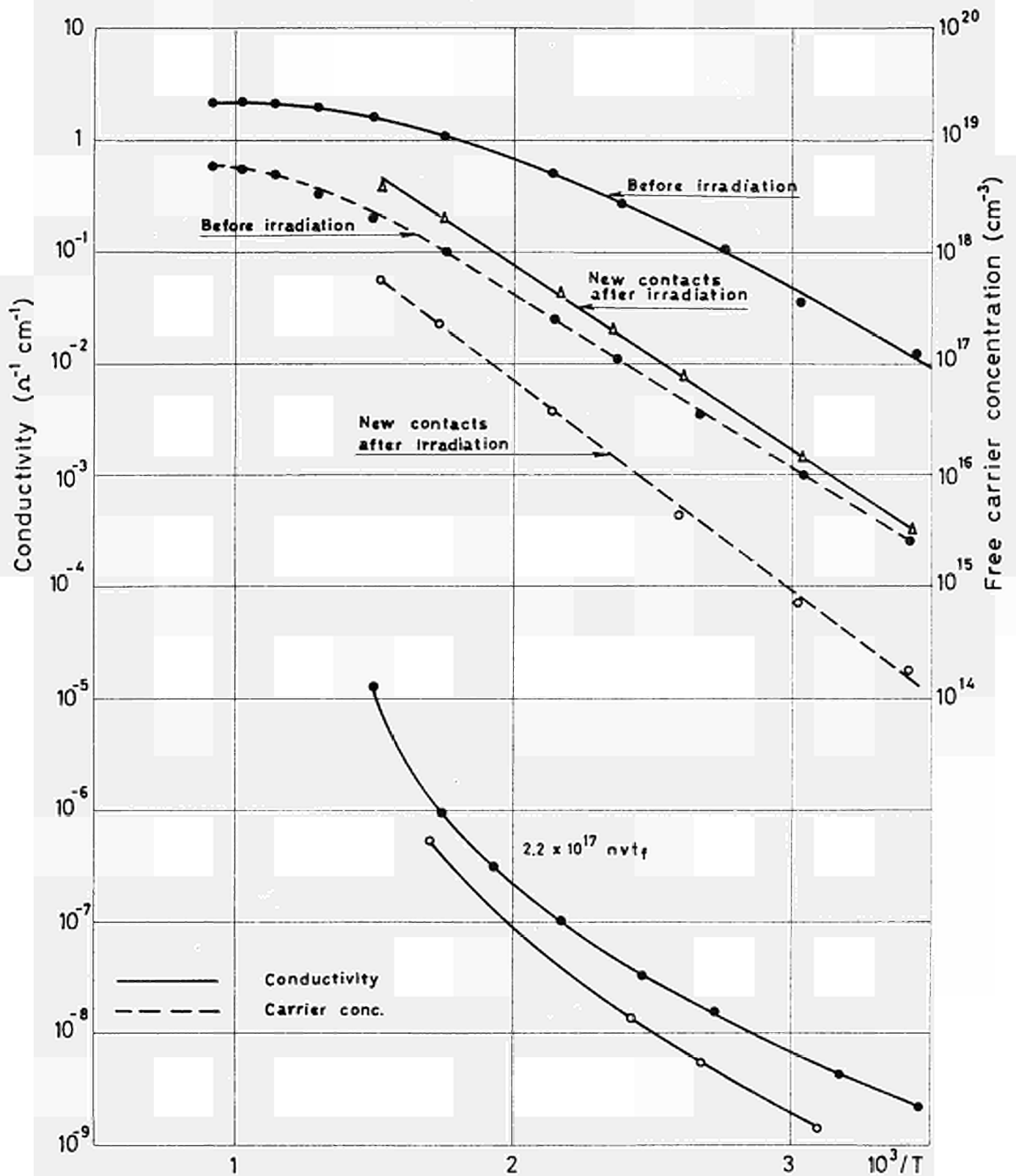
Fig. 29

Conductivity of p-type SiC as a function of temperature
before and after irradiation and with new contacts.
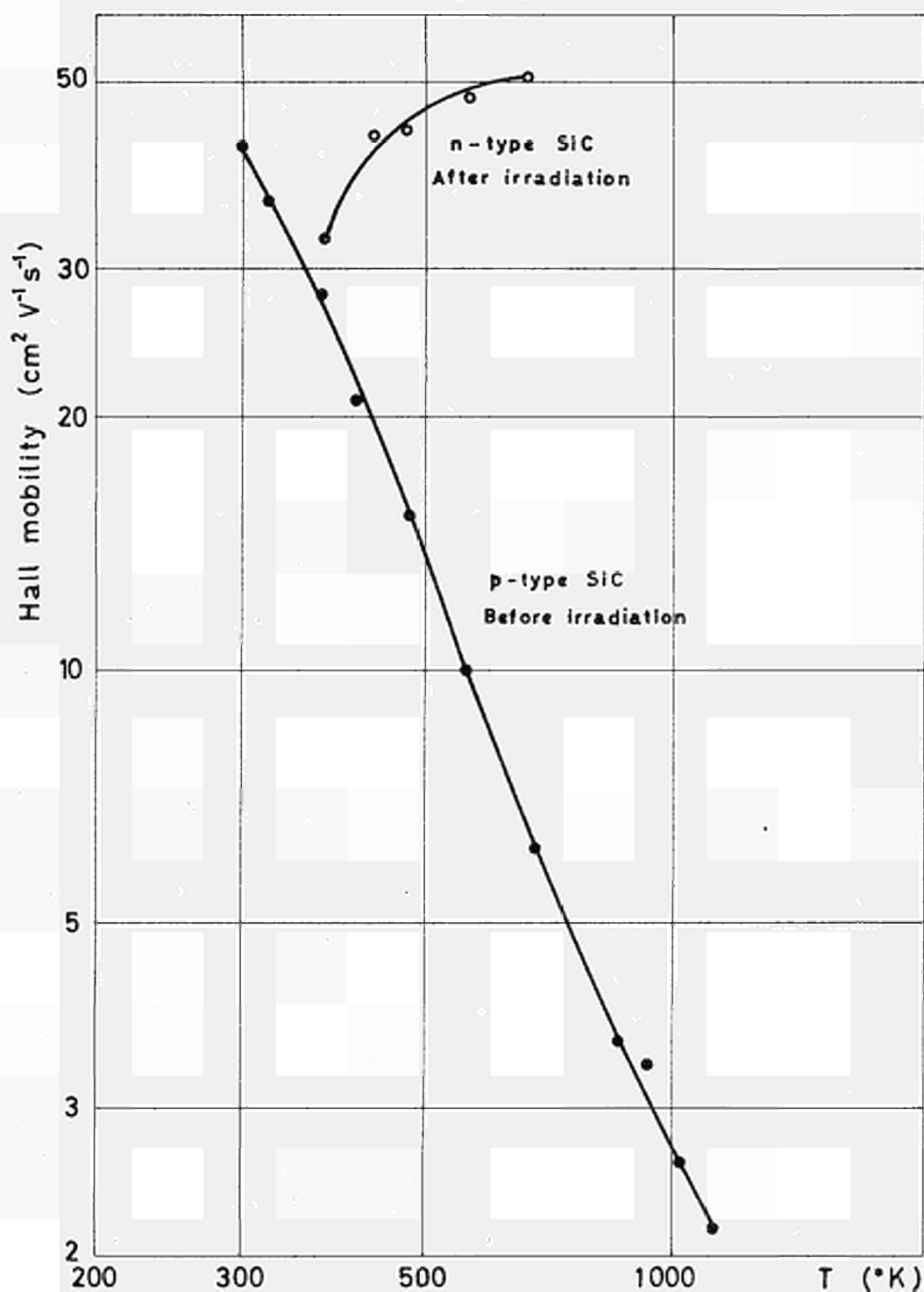
Fig. 30

Hall mobility of p-type SiC as a function of temperature
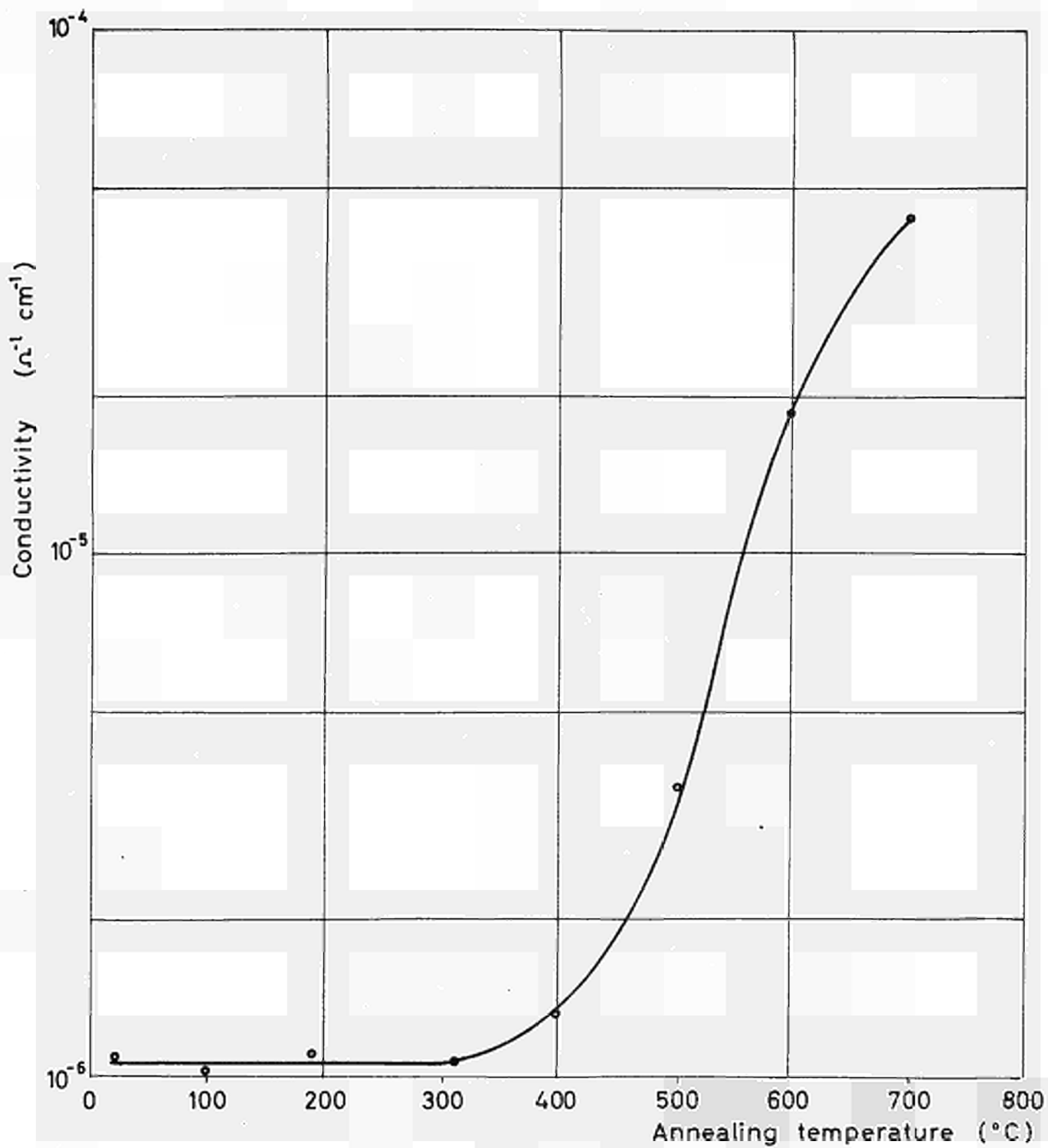before and after irradiation.

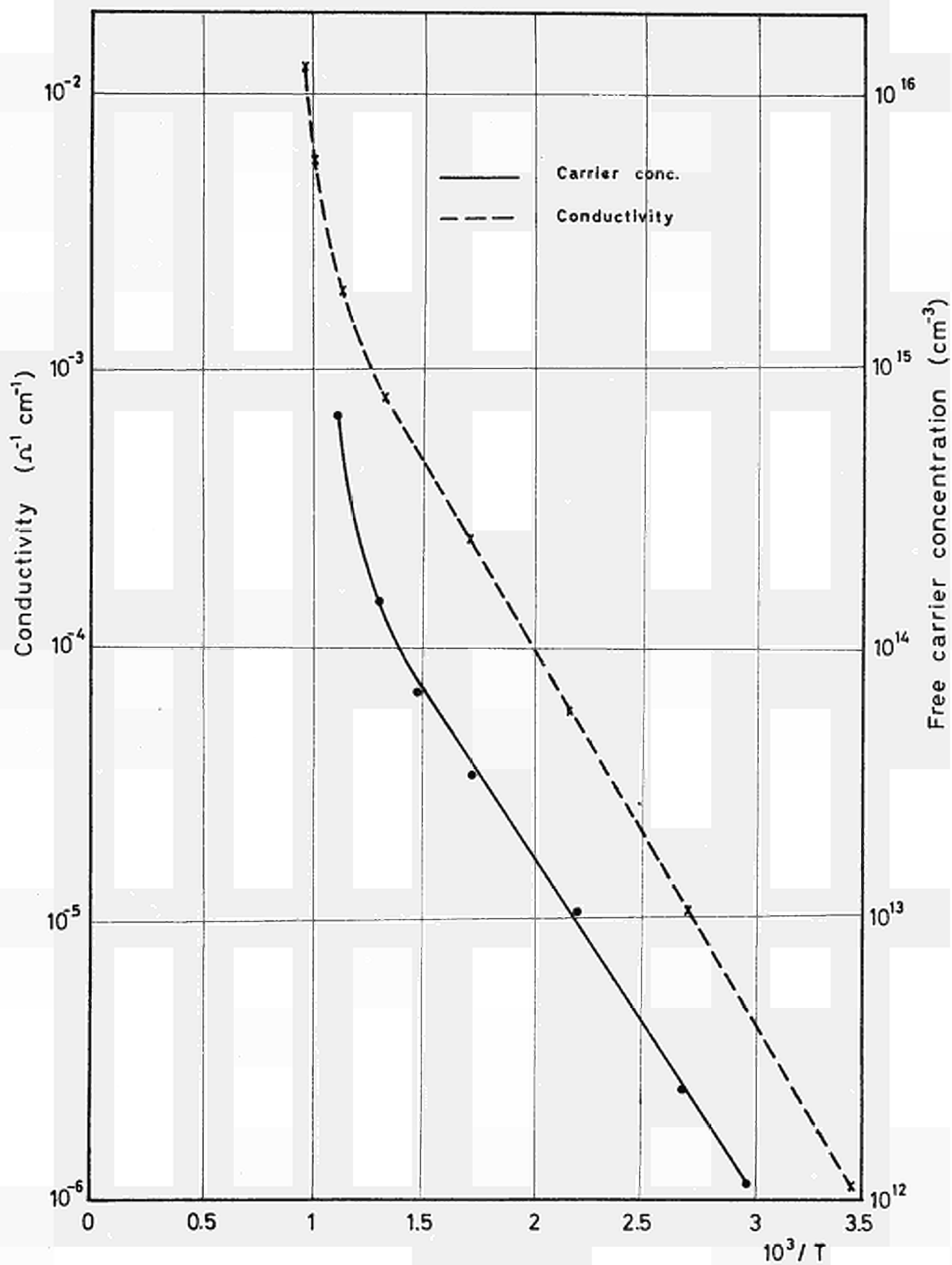Pulse annealing curve of p-type SiC after neutron exposure.
Conductivity as a function of temperature.

Fig. 31

— temperature curve
--- conductivity curve
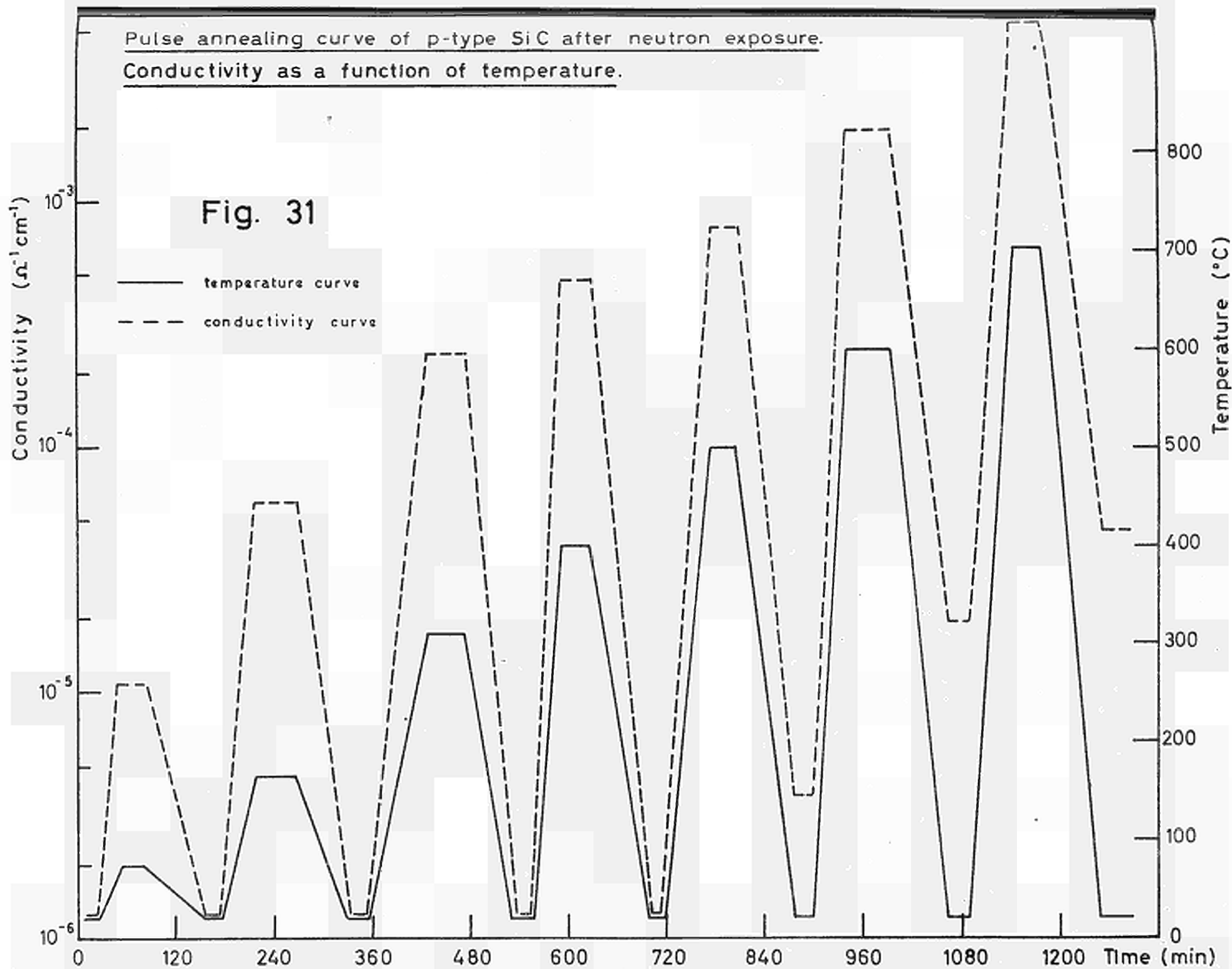
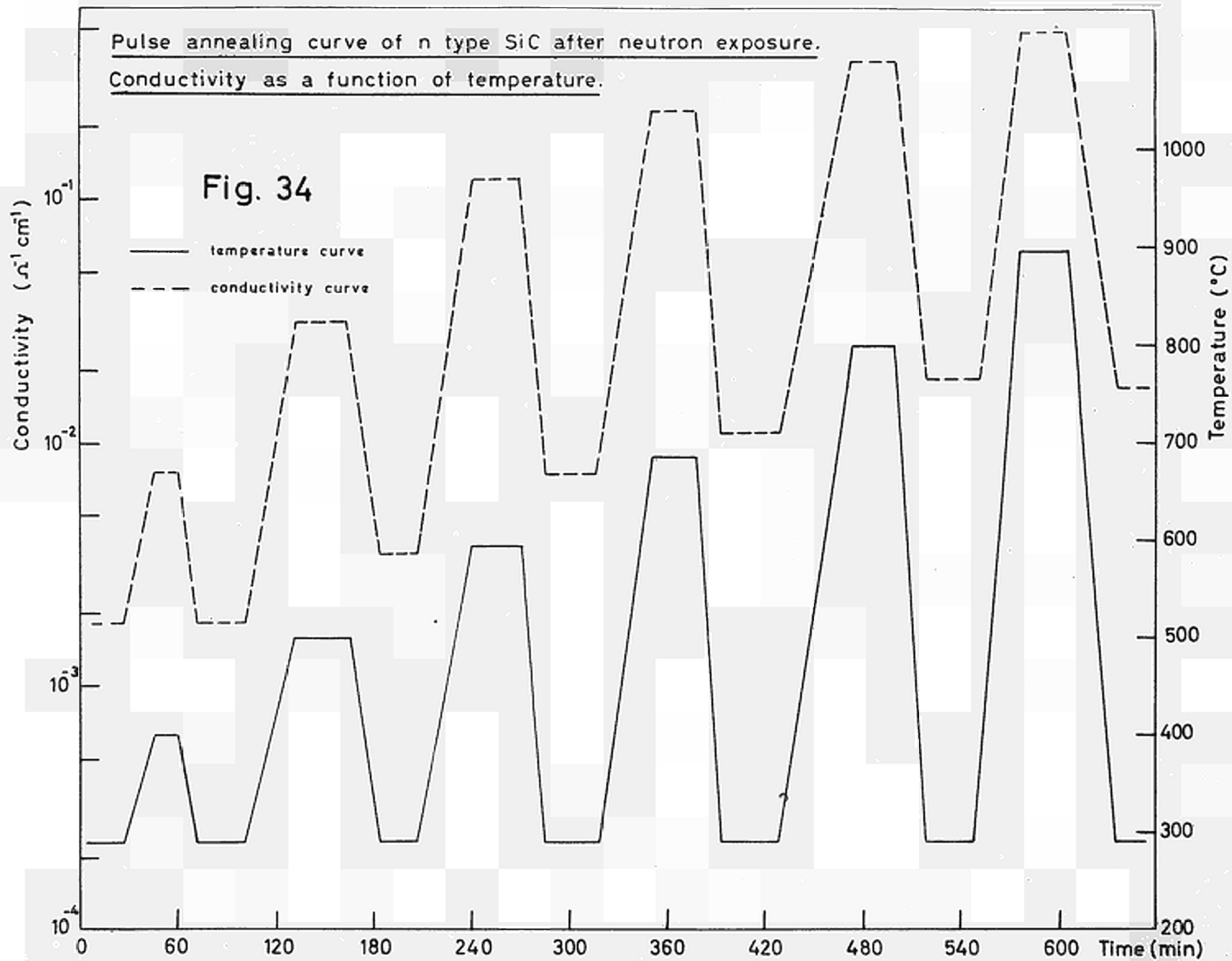Fig. 32.

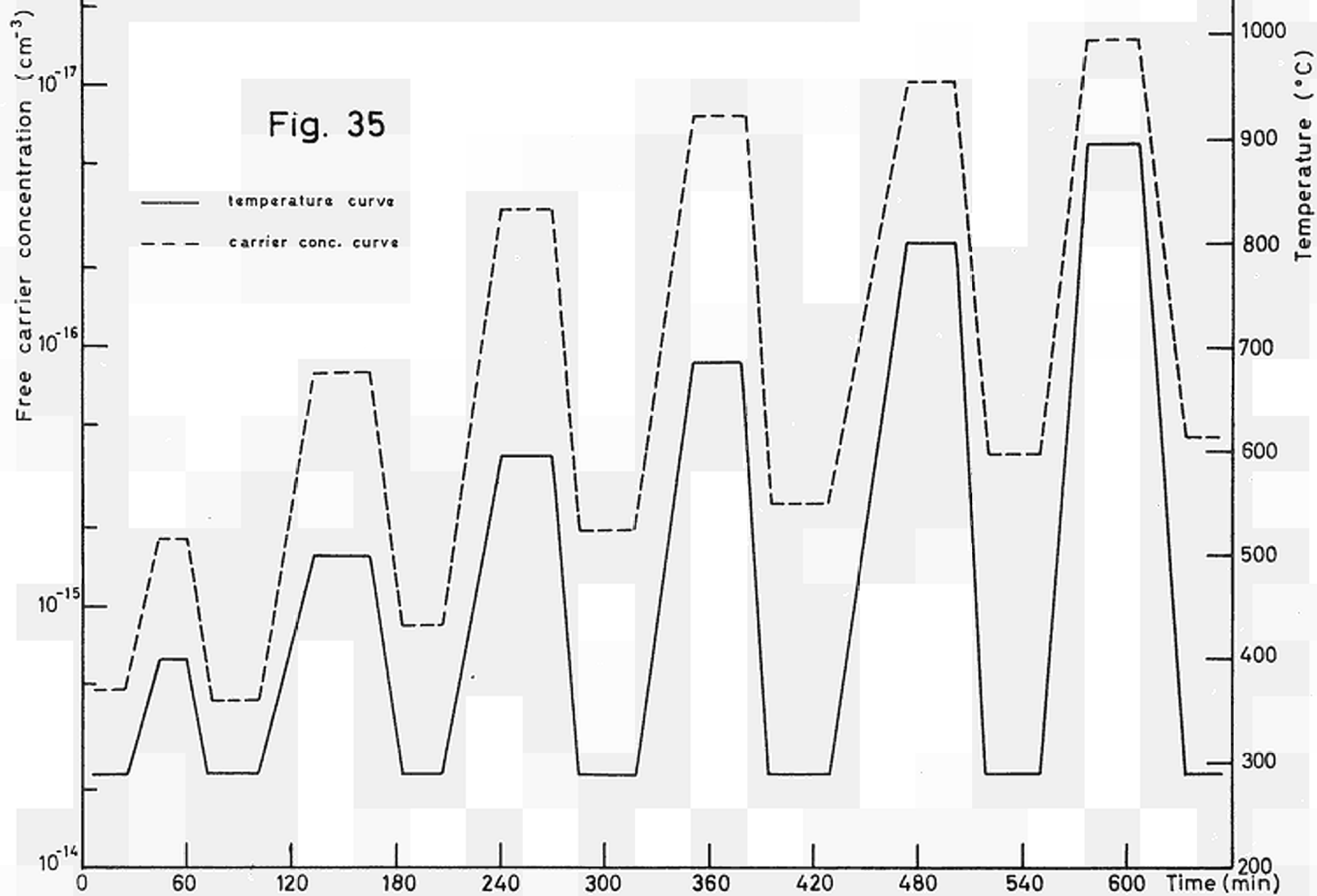Recovery of conductivity in p-type SiC after neutron exposure.

Fig. 33

Conductivity and free carrier concentration of p-type SiC at pulse
temperature.

Pulse annealing curve of n type SiC after neutron exposure.
Conductivity as a function of temperature.

Fig. 34

temperature curve
conductivity curve

Pulse annealing curve of n-type SiC after neutron exposure.
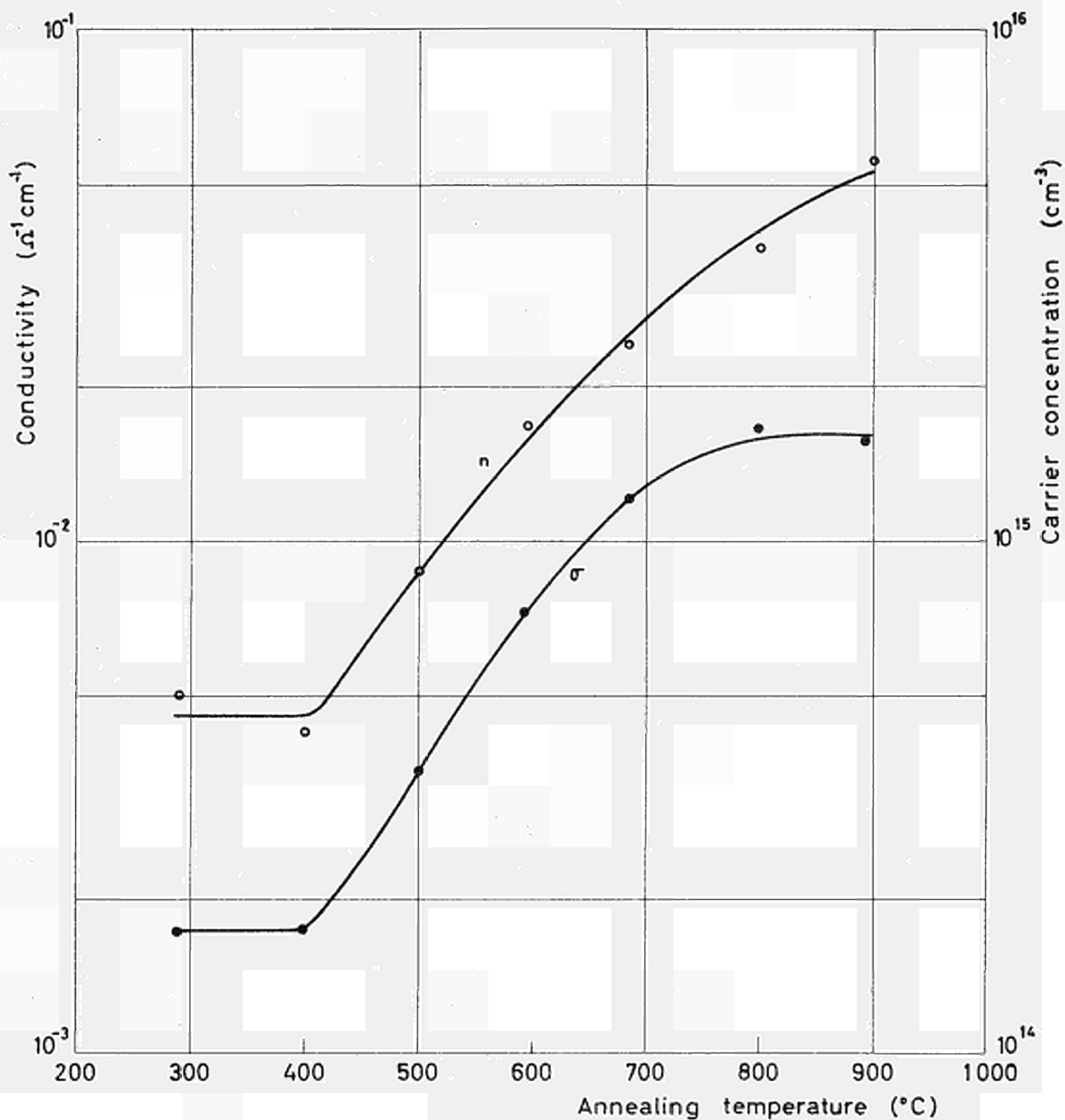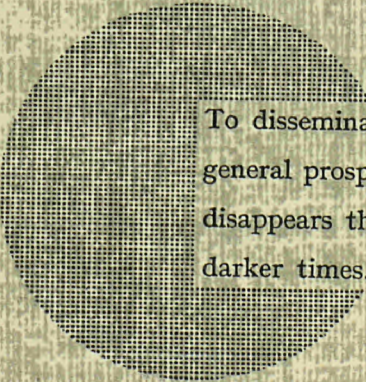Free carrier concentration as a function of temperature.

Fig. 35

Fig. 36

Recovery of conductivity and electron concentration
in n-type SiC after neutron exposure.

To disseminate knowledge is to disseminate prosperity — I mean
general prosperity and not individual riches — and with prosperity
disappears the greater part of the evil which is our heritage from
darker times.

Alfred Nobel